1.6 MHz Sonofusion Measurement and Model

APS '07
Roger Stringham, First Gate Energies, 4922 Akai Pl., Princeville, HI 96722
Jan. 20, 2007

ABSTRACT

Years of data collected from First Gate's various sonofusion systems gain fundamental support from recent extrapolations of hot fusion research. Consider the velocity, $3x10^4$m/sec, of a high density low energy jet plasma of deuterons that originates from the collapse of the TCB, transient cavitation bubble, in D_2O that implants a target foil [1 - Many ICCF & APS]. The foil generates heat via DD fusion events that produce ^{4}He and T. We compare our sonofusion to the jet plasma of Tokamak type plasma fusion systems with all their stability problems. Since sonofusion is a compilation of billions single fusion events per second and not a continuous fusion system like Tokamak, Stellarator, and Jet fusion systems; a comparison gives sonofusion a decided advantage. Also consider the relevance of the imploding wire and fiber technology where the MHD, magnetohydrodynamic, pressures exceed the crystal forces that bind atoms in solid state conductors. These are the same compression pinching pressures that compress the micro TCB jet plasmas which operate on a much smaller physical scale. The compression pressures delivered to the jet plasma seem to be the same magnitude. Sonofusion is more like ICF, inertial confinement fusion but also differs in scale with probably higher plasma densities. Sonofusion's implanted cluster deuterons with a few massive vaporous lattice atoms provide a transient fusion environment for low energy DD fusion events. Applying the developments ICF and muon fusion technologies to the sonofusion TCB jet plasmas makes some aspects in the comparison between hot and "cold" fusion more understandable. One hurdle our system must adjust to is that our measurements show there is no long range radiation (gammas or neutrons) and the main channel for nuclear DD fusion products is the ^{4}He channel. These problems are addressed via coherence in the implanted high density, transient, deuteron clusters. One can also apply transient BEC and Fermion theory to models of the implanted clusters. Finally, these sonofusion systems should be viewed as a beginning replacement for hydrocarbon fuels.

INTRODUCTION

Measurements of 1.6 MHz systems and applications of hot fusion technology to sonofusion are reviewed. Results from data collected in the early years are combined with more recent high frequency sonofusion systems. These results have been examined and compared to hot fusion plasma systems. The comparison leads to a more confident realization that sonofusion is in fact on a much more solid footing than in the past in the sense of an explanation of its fusion products. The picosecond sonofusion density environment is comparable to that of muon fusion [2]. The data from calorimetric heat measurement from the 1.6 MHz sonofusion device still needs the supporting analysis of fusion products found at the lower frequencies. For the present, we depend on the extrapolation of fusion products found in lower frequency experiments (20 and 40 KHz)

to the 1.6 MHz and 2.4 MHz systems. No search for fusion products has been attempted.

The TCBs that form jets during their collapse are a well developed technology [3]. However, the jet plasmas are not a well known phenomena [4]. We develop a path for the high density low energy plasma during the last phase of the TCB collapse that is transformed into a jet plasma and has the characteristics of imploding wire systems [5]. An MHD compression pressure pinch effect of a magnitude large enough to cause the atomic lattice of a wire conductor to break down is extrapolated to fit the TCB jet plasma. The further compression of the jet plasma contents is expected in the dense jet plasma the jet progresses the D_2O. The dense jet plasma of deuterons and electrons are implanted into the target. The implantation picosecond coulombic separation of deuterons from electrons in the target lattice as coherent deuteron cluster, D_x^+, creates an environment for the fusion of deuterons. Several factors extend the fusion contact time between deuterons in the cluster. Electrons rush, coulombic attractive forces, to the cluster's periphery producing deuterium atoms that surround the cluster [6]. Some of the peripheral deuterons will combine with the mobile excess of electrons to combine with deuterium atoms, producing a heat pulse directed to the center of the cluster. In the center of the deuteron cluster a few deuterons may fuse to produce a large heat pulse, no gamma rays, and destroy the cluster with deuterons reverting back to D_2O. ^4He, a fusion product, in the lattice heat pulse is ejected into the cavitating D_2O and Ar mixture. The analysis of the collection of gases in and over the cavitating D_2O was done by mass spectrometry [7]. The fusion heat pulse vaporizes the lattice of the target foil and as it reaches the surface the contents of the pulse are ejected. The ejecta contents contained the products of fusion events, lattice atoms, deuterons, electrons and deuterium but mostly the incorporated heat pulse's lattice atoms [8]. The SEM analysis of the target foil shows many ejecta sites that are sized and counted; their population size versus their calculated energy at the time of ejection shows a maximum population around 100 nm and minimum energy of around 20 Mev [9]. It should be pointed out that the production of ejecta site is a continuous process and the target surface is in continual change during the cavitation exposure. The instant the process is stopped the surface is frozen for a leisurely analysis process. The path from the jet plasma formation to the ejecta site is reasonable but not the only path to DD fusion.

EXPERIMENTAL FOR 1.6 MHz (Series 1 A runs)

The experimental set-up was checked before a run. The pump and circulation system were checked for leaks and blockages. The line-up of the photomultiplier with the reactor window was checked. The Light Box was closed and tested by the photomultiplier tube, PMT, for light leaks. Ar was bubbled into the D_2O bubbler which purged air from the circulating D_2O. (SL is several times more intense when pressurized with Ar [10] Make sure air is circulating through the Light Box keeping it at a steady-state temperature. Make sure the meters and data systems are working. Check that the levels of D_2O and H_2O in the bubbler and in the coolant bath are correct. Make sure the Qi pulsing system is set. Turn on pump and check temperatures, pressures, and flows for correct values. Turn on the sonicator to start the of Series 1 A experimental runs.

The path of the D_2O circulation system starts with a rotating piston FMI pump that pumps the Ar saturated D_2O through 1/8 inch stainless steel tubing to a sintered 20 micron stainless steel filter. The pump is a variable flow direct drive pump and maintains a constant D_2O flow with regard to mass flow of D_2O for a given setting. The D_2O flow continues through the stainless steel frit filter and past the Tin thermocouple at the input port of the sonofusion device. This is where the D_2O cavitation jet implantation, fusion heat pulse ejecta, and calorimetry occur. The reaction volume of 1cc has a D_2O residence time of about 0.92 cc/sec and is exposed to Qa, the acoustic input, for that time period. The D_2O passes out of the reactor at the exit port and a TC measures Tout from the sonofusion reactor. Tout – Tin, is the ΔTss for the cavitating D_2O flow rate, FR, and determines the heat out, Qo. Qo is the total heat measured that originates from the acoustic input and excess heat Qx in the sonofusion device. The flow continues through a ten foot 1/8 inch stainless steel coil where D_2O heat is exchanged into a 3.5 liter H_2O heat exchange bath. From the cooling coil the D_2O circulation flows to into a flow-meter, FR, that measures from 15 to 100 cc/min.and then into the bubbler where one atm. of Ar is bubbled into the circulating D_2O to saturation. The cooled D_2O is drawn again into the FMI pump as the circulation process continues. See figure 1, the circulation system.

A 20 gm sonofusion device has the window perpendicular to the earth's surface in its running mode. The device is a stack of concentric elements squeezed together. Ar pressurized D_2O is circulated through the 1 cc volume device by a FMI pump. The two electric leads are from the 1.6 MHz oscillator and power the piezo that is the acoustic input, Qa. The carbon fiber composite base plate provides a seal by squeezing the Neoprene piezo holder. The base plate is squeezed against the window and base plate making the device water-tight. The polycarbonate window allows for the PMT photon counting. A target foil is held tightly and acts a shield for the window blocking most of the cavitation activity and photon emission from the window. See figure 2. The materials of the sonofusion device construction were of assorted plastic parts to maintain its low mass. This limited the pressures that could be used in the device. The heat loss to the environment via convection was low because the difference between room temperature, RT, and the steady-state temperature of the device, T ss, was relatively small, ΔTss. With these conditions only a small part of the device heat was lost to convection while the majority of the heat was removed by the circulating D_2O where the watts out, Qo, at steadystate equals (ΔTss)(Flow)(4.184) in watts. Qo includes Qa and any Qx produced. Keeping the mass and ΔTss of the sonofusion device to a minimum reduces the heat lost via convection.

After checking the data collection for consistency including temperatures, flow, photon emission, and pressure, the run input power from the wall, Qi, is connected to start the run. The power is pulsed on and off for intervals of thirty or sixty seconds. For each on-interval the system's heating curve approaches at least 95% of its steady-state temperature of continuous running and for each off-interval a cooling curve is produced for circulating the D_2O. In this mode the heating and cooling curves, HC and CC, data is collected and examined for RF, radio frequency, interference after the run. Looking for

deviations in HC compared to CC gave me assurance that RF was not a ΔTss determination problem. See figures 3 and 4 for the plot of Qi, Qx, and SL and the resultants linearity after SL is noted. The low mass of 20 gm sonofusion device allows for the rapid ΔTss and heat measurements (the mass flow heat content of D_2O is more than the 8 times that of the 20 gm reactor for the ΔTss). The data ΔTss is recorded by in and out with K type thermocouples. One must be careful not to measure temperatures too near the input and output reactor ports as heat conductance from the reactor that is at a slightly higher temperature may interfere with those measurements. These problems can be handled by measurements using a calibration Joule heater in the sonofusion device. See tables figure 4 and a more detailed data list in figure 5 table.

The flow through calorimetry is composed of the product FRxΔTss in calories and involves a compromise between (high FR and low (ΔTss)) and (low FR and high (ΔTss)). This is a simple path for calculation of the steadystate watts out, Qo, of the sonofusion device, which includes any Qx produced. There are some device heat losses that should be investigated that are not directly measured, specifically the convection loss from the surface of the sonofusion device at Tss temperature.

RESULTS OF Series 1 A runs; 1.6 MHz EXPERIMENT

Figure 3 shows the resultant, purple line, of three parameters (excess heat Qx, watts input Qi, and sonoluminescence SL) measured during experiments. The data was collected for Runs of Series 1 A and is shown in figure 4 table. These experiments were made using a low mass 1.6 MHz sonofusion device. SL measurements indicate the presence of a high density partial plasma from the collapse of TCBs in D_2O. The sonofusion parameters need to be adjusted and controlled to produce SL, which is measured via a photomultiplier, PMT. Its presence is necessary and indicates a Qx production environment. The TCB collapse process produces jets during the last stage of the bubble collapse. These jets contain D^+ and e^-, a plasma, that is accelerated into a metal target, implanted, where sonofusion takes place producing Qx. Qi is the 60 cycle input from the wall which is split between Qa, the acoustic input, and Qos, the 1.6 MHz power oscillator. The acoustic input to the sonofusion device Qa equals 0.33Qi, the efficiency of the sonofusion device's acoustic production.

One can see in the data gathered for figure 4 Table from the sonocation circulation of D_2O through the 1 cc volume of the sonofusion device, that when the Qi is increased by the use of the controlling variac from zero to around 15 watts (a Qa of 5 watts) there is little SL or Qx. As Qi continues to increase, there is a break in the resultant and it proceeds in a straight line in an upward direction with an increased slope and increasing Qx production. This initial low input response is understandable as Qa at first produces only acoustic waves and heat in the D_2O but no TCBs. No acoustic cavitating bubbles in the TCB energy range and no Qx watts are produced until a Qa threshold of 5 watts power level is reached. The working pressure in the sonofusion device is about three atmospheres. As the acoustic amplitude of Qa increases, Qa = .33Qi, TCBs start forming. TCBs selected from this cycle of bubbles population will collapse forming high density plasma jets and will implant into the target foil producing fusion events and Qx. Further increase in Qa acts to cutoff TCB formation as bubble frothing starts occurring.

This can be controlled by reducing the temperature or increasing the Ar pressure. In this system bubble frothing starts with a Qi around 130 variac volts (a Qi of 43.4 watts and a Qa of 14.5 watts) and originates from a household 120 volt power line. The primary parameters that control TCBs are device pressure of Ar, temperature or vapor pressure of D_2O, and acoustic power input, Qa.

The three critical parameters above are adjusted to create the TCB producing environment in the sonofusion device. Another factor important to control is the monitoring of Qx production that is coupled to the SL intensity production from the TCB collapse process. So we have added the SL parameter that monitors the SL photon count via a PMT. There is always the geometry of the reactor, the flow, sonofusion device exit orifice for D_2O, the method of extracting heat, and the resonance frequency of the reactor that need to be considered. These coupled parameters and their relative magnitudes are important in producing Qx. Once all these factors are known and understood, the complexity of a sonofusion device can be reduced to simple basics and be more dynamic with respect to high temperature and pressure. Figure 5 is a more complete table of the spread sheet data gathered from runs of the Series A experiment.

CALORIMETRY

The calorimetry used for the Series 1 A experiments was simple with some limitations. The measurements of heat out, Qo, to determine the ΔTss of the circulating D_2O and the flow rate, FR, of the D_2O through the sonofusion device. Also the use of the heating curves and cooling curves, HC&CC, from Newton's Law of Cooling is essential. The Qo = (ΔTss)x(FR)x4.184 watts without correction for heat lost via convection. It becomes less accurate as the delta temperature at steadystate, ΔTss, and increases as the FR decrease. These two measurements, temperature and flow, should balance as one depends on the other for best value regarding their error factor. An adjusted FR of about 55 cc/min, a middle value, is a good compromise. The errors of under-measurement are heat losses that increase with increasing ΔTss and are of a radiative and convection nature (radiative losses in the low mass device are negligible). So the flow through calorimetry method is always going to register a low value for (ΔTss). Water flow rate could also be a problem as D_2O flows were calibrated with light-water flows and volume measurements. The D_2O viscosities are slightly higher and the density is 11% higher. These are compensated for by using a pump that takes a known volume of water and injects it into the circulation line creating a circulating flow so the flow is based on volume and is unrelated to mass or viscosity. The temperatures of the D_2O flow into and out of the 1cc sonofusion device were measured by K type thermocouples. Several other thermocouples were placed at positions of interest. The data was collected and plotted via "Computer Boards Inc." PCI-DAS-TC board in a PC that dumped data into a Microsoft Excel spread sheet. Check 12 min. video and paper from [11].

A part of the calorimetry is the check for radio frequency, RF, interference in the thermocouple measurements and data presentation in a graphical form. This is done by examining a cooling curve, CC, from the data of the run and then rotating it 180^o around the x-axis. The CC is compared to the heating curve, HC. If it matches, it is OK as is. If it does not match, the appropriate subtraction can be made from the HC to get a match

with the CC. The CC will have no RF interference as the 1.6 MHz driving piezo is off. A number of CC and HC are produced during each run of the Series A experiment. See data in the form of consecutive HC and CC in DVD of the sonofusion device [11]. There are cases when the data of the HC is too distorted by RF and the data is no good, but this was not the case for the Series A experimental runs. The ΔTss is determined by the RF corrected HCs.

For example in the Series 1 A, run #6, the sum of convection and radiation losses were under 2 watts with a Qa of.16.6 watts, a Qx of 38.2 watts, a Qi of 50.4, and a Qo of 54.8 watts. So the error for the Δ Tss measurement was 2/54.8 which is 3.6% under the real value for Qo. The flow that was delivered by an FMI pump is not influenced by viscosity or density and delivers a constant flow due to its synchronous rotation and reciprocation of its piston. A piston revolution is required for each suction/discharge cycle giving a pulsed input to the flow in the circulation system. The pump's pulse rate is about 10/sec for a flow of 55 cc/min. through the sonofusion device. A more detailed calorimetry description is a work in progress.

ACOUSTIC POWER DISTRIBUTION & Qx

The acoustic power input to the sonofusion process is a very inefficient process. In the sonofusion device the distribution of input power, Qi, is divided between the Qa and Qos where Qa/(Qa +Qos) is the efficiency of the sonofusion device. The geometry of the device also plays an important part in its efficiency. The disk volume of the cavitating D2O and the target placement emphasizes the maximum target exposure to plasma jet implantation.

The 10 amp. variac controlled input from 0 to 140 AC 60 cycle volts delivered to a transformer and rectifier 55 volts DC to the 1.6 oscillator. The 1.6 MHz signal input is in a 120 Hz envelope so covers a range of voltages, some of which will have values that produce TCBs. The variac input Qi can be slowly increased to establish the first appearance of SL. A continued increase in Qi will produce a maximum for SL; then with a further Qi increase SL will drop as most of the bubbles will burst rather than collapse because Qi is too high for the reactor running pressure and temperature. This is a good policy to follow until more is understood about locating a sweet-spot voltage that is coupled to the parameters temperature, pressure, and acoustic input - the optimum to produce maximum Qx. This range of voltages tends to smear the information obtained from the experimental runs regarding the best choice of parameter values, but as long Qx is produced, we have some of the relationships between parameters in the neighborhood of useful voltages. See figure 6.

An example of sonofusion activity was the experimental set-up that included 11 runs of Series 1 A experiment. The electric input from the variac varied from 30 to 140 volts at 60 Hz with a power input that varied from 2 to 50.4 watts for the Series 1 A runs measured by an Ohio Semitronics Inc. wattmeter. Some of this Qi input was used to power the 1.6 MHz oscillator, Qos, and the rest (the oscillator output) powered the 1.6 MHz piezo, Qa. The oscillator converted 140 to 30 volts via a transformer to a DC input for a LRC Class 1 oscillator with a square wave transducer. The 1.6 MHz input

amplitude to the piezo varied in a 120 Hz envelope from zero to a maximum voltage measured by an oscilloscope. For example in Run 6 of Series A; 140 AC 60 cycle volts driving the LCR class 1 oscillator at 1.6 MHz at an acoustic input produced a, Qa, of 16.6 average watts (0 to 23 watts). The 16.6 watts of Qa delivered to the 1.6 MHz piezo was delivered to the sonofusion device driving the piezo produced heat via, acoustic waves in D_2O (frictional heating of D_2O) and creation and collapse of TCBs. Further heating of D_2O is the distribution of acoustic power into the sonofusion device; heating the target foil via acoustic absorption, heating the SL window by absorbed acoustic power, heating the mass of the reactor, and the heating via target implantation of deuterons into the target lattice producing DD fusion events and Qx. The measurement of Qx was that heat above the Qa 16.6 watt input. In this example Qx was 38 watts and Qo was 54 .6 watts. Heat generated in the sonofusion device was removed using the flow through of D_2O and its generated $\Delta Tss = Tss - Trt$. Tss was the steadystate temperature during sonication and Trt was the ambient temperature. ΔTss was kept low by the short residence time of D_2O in the sonofusion device via a high flow rate of D_2O. The heat generated in the reactor from Qa, and any produced Qx must be removed quickly from the reactor for good calorimetric measurements. Calorimetry at high ΔTss was not practical.

The quantitative distribution of the 16.6 Qa watts (in Run #6 of the Series 1 A experiments) is not definitively known but some educated approximations can be made for the watts used for producing the implanted target foils. The volume of D_2O is about 1cc so there are no SL or bubbles at one atmosphere external pressure until a level average 5 watts of Qa input is reached in the sonofusion device (Qi would equal about 15 watts) and this low Qa input is mostly the production of acoustic frictional heating of the piezo and D_2O. The mechanical flexing of the piezo via the 1.6 MHz accounts for 7 watts of the total of Qa 16.6 watts. Approximately 8 of the 16.6 watts goes to heat the target foil, sonofusion device, and D_2O via acoustic absorption. The window forms the external containment of the D_2O farthest from the piezo but would be quickly destroyed if it were not protected by the intervening target foil and may account for 2 watts of Qa heating. It is important to note that the temperature difference between target foil and piezo, (Tf – Tp), should be positive if Qx is being produced. The (Tss-Trt) is kept low which reduces the amount of convection loss. The higher the surface temperature the more heat is lost for calorimetric measurement.

The watts used to generate bubbles are determined from the column of water from a 1.6 MHz reactor, with the window removed, producing a continuous column of water 10 to 15 cm high and 1cm in diameter with a Qi of 37 watts and Qa of 12.2 watts. This is measured as a force $F = -mg$ (g is the acceleration of mass m at the earth's surface, and relates to about 1 watt of Qa that produces bubbles. The conditions in the sonofusion device are different with regard to pressure but serve the purpose of indicating the small amount of Qa that is actually used, around 1 watt, to produce bubbles. See figure 7.

From the modulated 120 Hz acoustic input about one watt of the 16.6 watts of Qa is available to produce bubbles of which only 1% are of the TCB acoustic bubble population that resonate to the 1.6 MHz frequency. This is not an efficient process. The reactor geometry further reduces the efficiency of TCB jet plasma target implantation, by

another factor of 1 in 100. These TCBs that produce jet plasmas within the range of the target are the ones counted for potential fusion events. From a Qa 16.6 watts only 10^{-4} watts or less are available to produce fusion events and Qx. An input of 10^{-4} watts produces 38 watts of Qx. See figure 7.

Looking at this distribution in terms of deuteron numbers is another approach to analyze the efficiency of the sonofusion process. The involved TCBs produced in the flowing and cavitating D_2O bubble production efficiency shows the following relationships. The 1 cc reactor volume of D_2O contains approximately10^6 TCBs/cycle, or 10^{12} TCBs/sec, and 10^9 implants/sec. to 0.25 cm^2 surface area of the target foil. The 10^6 TCBs per cycle will occupy 10^{-5} cc of the 0.25 cc acoustically active D_2O. The high density pinched jet contains 10^7 deuterons per implant with the potential to create 1 to 1000 fusion events/implant. From the data (See fig.11) an average of 10 fusion events occurs for each implant. So the number of fusion events found in ^{4}He found in the LANL experiments at $1.2x10^{18}$ (times) implant/sec. will produce 10^{13} He4/sec.and this converts (mc^2) to a Qx of 40 watts without the detection gammas or neutrons [12]. A gain or loss in any of these numbers will cause Qx to change accordingly. A Qa of 16.6 watts uses only a 0.01 watt to produce TCBs that only 1 in 100 will implant to produce Qx. That is only 10^{-5}x Qa watts that are involved in producing 38 watts Qx.

JET PLASMA AND COMPRESSION

The final stage of the TCB collapse process will produce a jet. The jet is given birth by the dynamics of the final collapse process of the TCB where the TCB's surface velocity of collapse of the bubble's interface with respect to its center is greater than Mach 4 [13]. A high density jet plasma is formed from the TCB contents and is ejected from the bubble surface several times faster than the bubble interface velocity of about Mach 20 or 3*10^4 m/sec. The sheath electrons of the jet of the dissociated contents, consisting of D_2O, D^+ and e^- of the jet plasma, produce a strong local electric and magnetic field directed towards and perpendicular to the z axis known as the pinch pressure effect. Actually, there are three compression pressures that complete P_c, and they are P_{ST} , P_E, and P_B. The pressures P_{ST}, surface tension and the P_E and P_B pinch compress the rapidly moving plasma contents to higher densities. These pressures give the observed tapered geometry to the jet plasma depicted in the many photos of these transient phenomena [jet photos]. This compression pressure is larger than the escape pressure, $P_{es} = nkT$. We can make reasonable estimates looking at photos of jets in the KHz range and extrapolate to bring values to the jet plasma in the MHz range which includes their size, geometry, density, and velocity. Much of the information from known KHz references and experimentation will apply to MHz systems of TCB jet plasmas.

The TCBs formed at 1.6 and 2.4 MHz experiments have characteristics extrapolated from 20 and 40 KHz systems and are the following [10]. First is the selection of a 0.4 micro meter initial radius bubble Ri from the residual initial bubble population during the negative and growing phase of the acoustic cycle. The content of the Ri TCB was about $2x10^7$ molecules of D_2O + Ar (Ar will increase the energy density in the TCB through its polytropic constant during its collapse in the acoustic field). The isothermal expansion of the TCB Ri coupled to the piezo input expands the bubble to its maximum radius, Ro, of

4 micro meters and increases its mass content via rectified diffusion of D_2O + Ar by evaporation and aerosol ripped from the bubble's interface. At this point the TCB at its maximum radius, Ro, is partially evacuated with its increased contents of $3x10^9$ of D_2O + Ar. The pseudo adiabatic collapse of the TCB to the final radius, Rf, of 0.03 micro meters bubble with a final bubble content of 10^9 D_2O + Ar ends with an SL display of photons. The jet plasma formation finishes the TCB collapse cycle in one acoustic cycle (wave) with a high density low energy plasma content of 10^7 D_2O, D+ and Ar. This transient jet plasma will implant into a target foil and is actually a high density deuteron accelerator. There is loss of bubble content during the collapse process while it is organizing the bubble's D+ and e- contents into a unidirectional system as the jet plasma is formed leaving behind most of the D_2O, Ar and O. The unionized deuterons from the partial plasma are stripped of their single e- via lattice impact stripping and may join the other D+ present.

The spread and velocity of the electrons and ions leaving the TCB under the influence of the TCB interface as the jet plasma contents are defined by the geometry, interface, and Pc – Pes into the characteristic conical jet plasma. The path length and duration of the plasma jet in D_2O is determined by the pinch mode. The last phase of the TCB's extending interface to the jet plasma's birth involves the natural flow of both the outside and inside of the TCB interface to form the jet plasma containment. The central top TCB interface surface becomes the interior wall and the central bottom TCB interface becomes the exterior wall of the hollow jet plasma. A hollow core of the jet plasma gained from the TCB interface by the jet plasma's internal surface is an inner sheath of electrons with possibly a core of electrons that add to P_{JxB} compression of the plasma. The profile cross section through the jet plasma cone is of the donut cross section geometry. See figure 8. The distribution of the pinched plasma contents in the hollow cone geometry is in continuous compression density change with the P_c influence being highest at the tip where pinched densities may match those of white dwarf stars ($3x10^{35}$ m^3) [13]. During the jet plasma's short lifetime the dynamics within the plasma are astronomical. P_c compression of the jet plasma's contents produces a density and pressure gradient along its length.

With most of the D_2O, Ar, and O ions excluded from the jet plasma due to their high mass-to-charge ratios, these ions can be stripped from the plasma, the initiation of the jet plasma. The velocity is around $3x10^4$ m/sec and the initial volume is $2.6x10^{-24}$ m^3 and produces a jet plasma content that consists mostly of D^+ and e^-. For example the plasma contents which are initially at a density of 10^{31} deuterons/m^3 in the jet plasma volume, figure 10, will be compressed to higher densities by the electro-magnetic pinch. The jet plasma volume contents are a plasma projectile (a D^+ accelerator) of the TCB. The jet plasma takes the form of an elongated cone with a base radius of $3x10^{-9}$ m and a length of $90x\ 10^{-9}$ m. As an example there is a sheath current at a density of n^{31}/m^3 where a current of 1.36 amps produces an increasing transient compressing P_c, the jet plasma compression pressure, with these conditions produces a B around 90 Tesla in the jet plasma. The estimate for sheath electrons in this example is 10^4 for N with n^{31}/m^3as the density. The P_c will rapidly increase as the jet plasma heads towards implantation. It will continue to increase until the jet plasma is pinched off or implants. There is an initial

rotational frequency associated with the sheath electrons that are around $6.3x10^{13}$ cycles/sec. The $P_{ST} = 10^{11}$, $P_E = 10^{13}$, $P_B = 10^{10}$ and $P_{es} = 10^{12}$ J/m^3, the jet plasma escape pressure, that shows that the jet plasma is in a high compression mode. With the ratio of P_{es}/ P_c much less than 1.0, the plasma jet in this example is being compressed. As this ratio becomes smaller, the plasma is squeezed with more force adding density and velocity to the jet plasma. A further speculation is that the birth of the jet plasma has an evacuated hollow core. See figure 8. This core may be filled with higher velocity sheath-like electrons that add to the total compression force. Increasing the temperature of the jet plasma contents is not going to have much influence on the stability of the jet plasma.

The larger ions of deuterium-oxide, oxygen, and argon may reside in the back end of the plasma (the more massive ions may be pinched off at the jet plasma formation) with their high charge to mass ratio and those ions are blocked by the massive target lattice atoms from involvement with implanted D_x^+ clusters. The jet plasmas that do not implant will terminate via a zipper effect starting at the point of the jet plasma.[13]. It is of interest to note that most of the sonofusion jet plasmas produced will terminate without implantation. The increasing density in the plasma jet as it is magnetically squeezed particularly near the tip of the plasma may reach a point where DD fusion can occur by increasing the density by a couple of orders of magnitude. The jet plasma system will have the density of muon fusion system. Remember that there is no need for the sonofusion's jet plasma to produce a self sustaining fusion system to be a successful power generator. Each TCB jet plasma is a separate fusion machine that is produced and ends in one acoustic cycle. There are millions of jets produced in each acoustic cycle.

PINCH

During the TCB collapse process, it is important to consider the connection of the interface and the plasma sheath that are rapidly evolving one into the other. This is the containment skin for both the TCB and the jet plasma. The z-pinch phenomenon which is the squeezing or compressing of the collection ions and electrons (charged particles) moving as a unit (a dense plasma) with a known velocity induces electric and magnetic fields with a resultant pressure, P_E and P_B. The pressures that create the z pinch in jet plasmas are electro-magnetic, and have been studied in great detail starting in the 1950s particularly for their application to hot fusion systems. The pressure P_E and P_B are directed perpendicularly to the center of the jet plasma velocity path and is part of the overall jet plasma's compression pressure ($P_c = P_{ST} + P_E + P_B$) Each TCB jet formed is subjected to the P_c pressure that overcomes the escape pressure, P_{es} and these two pressures shape and confine the jet plasma. P_{ST} in the jet plasma is that of surface tension at the jet plasma interface skin where the D_2O is the interface of a very small jet plasma cavity via hydrogen bonding. (In the collapse process of the TCB skin is the interface of the bubble contents.). The electric and magnetic fields share the energy density effects in the compression of jet plasma contents. The E field pressure is the plasma generated electric field from sheath electrons in the form of a capacitance. The B field contributes pressure from the jet plasma high velocity electrons $F_B = JxB$ that produces kinks in jet plasmas, and adds to terminating effects of the electric field. The escape pressure P_{es} is just nkT for the jet plasma and the temperature assumed for T is 10^4 ^oK. High density jet

plasma micro scale one cycle sonofusion processes are similar to hot fusion processes that are also one cycle processes like Inertial Confinement Fusion, ICF. The implosive wire process, and the muon fusion process, MF, although a catalyzed process can also be viewed as supporting a continuous fusion events as a chain reaction with densities an order of magnitude higher than sonofusion. These are different from the continuous fusion processes which use magnetic confinement of plasmas in Tokamak and Stellarator reactors, which fail because pinch problems do not allow for a continuous fusion operation. It is this same pinch process that makes the sonofusion process work. The value of P_c always exceeds the value P_{es} as the D^+ density increases giving transient stability to the jet plasma. P_c, the pressure of compression composed of the pressure of, $P_{ST} = 2\gamma/r$, ($E= N_s q/(4\pi\varepsilon_o)$, and $P_E = k_e(Nsq)^2/(Ar'^2)$; $B = \mu_o/2\pi\,(I/r)$ and $P_{JxB} = N_sq(v_dxB)/r^2$ are balanced against $P_{es} = nkT$. See figure 9 for the relation between P_c and P_{es} and the Appendix.

F Electro or magnetic force

μ_o Permeability of free space

ε_o Permittivity of free space

N_s The number of electrons that forms the jet plasma sheath

k_e The coulomb constant $(1/4\pi\varepsilon_o)$

I The Jet plasma current in amps = nqv_dA (q is the charge on the electron and v_d is its drift velocity)

Q N_sq the capacitance charge

v_d The velocity of the jet plasma

r The radius of the jet plasma base in meters

r' The average distance of the skin (the jet plasma interface with D_2O)

A The surface area of the conical jet plasma

n The density of electrons in plasma jet particles in m^{-3}

k The Boltzmann constant

T The absolute temperature of the jet plasma

τ The necessary confinement time for a fusion event to occur

γ The surface tension constant of D_2O is 7.2 in SI units

P_c is greater than P_{es} as the jet plasma increases in density. The pressure ratio between these two is less than 1 and will compress the jet plasma and its contents in the conical containment geometry shown in photos [14]. As "n", the density D^+/m^3, increases so do P_c and P_{es}. P_c is a function of "n^2" in P_B and P_E where P_{es} is a function of "n^1" [15]. If the plasma implants the target, there is a good chance for DD fusion to occur. (Of course there is always the possibility of fusion occurring in the z-pinch plasma if "n" is large enough. A short discussion of this possibility is found at the end of this subject.) If the jet plasma does not implant, it is out of range of the target foil. It will self-destruct in the cavitating D_2O via the z- pinch compression, sausage and kink mode, where the jet plasma contents will revert back to D_2O. The TCB collapse process creates an environment that fits the Lawson's criteria $(n*\tau*T)>10^{21}$ for sustained fusion events, which sonofusion is not. There is no necessity for sustained fusion in the sonofusion process $(10^{31}*10^{-12}*10^4) = 10^{23}$ a number above which DD fusion can be self-sustaining (Lawson's Criteria). This is a characteristic that is not necessary in sonofusion as it is a <u>one time event</u> or one cycle event for the TCB and deuteron accelerator sonofusion

system. The fusion event(s) destroy the transient cluster of deuterons (the birthplace of fusion and the fusion environment). The energy is released as heat instead of the production of the 24 Mev gamma and further fusion events for that particular TCB and implantation events are finished.

The jet plasma's geometry is derived from forces initially established in the TCB collapse and its interface. The dynamics in the plasma involving drift current, electro-magnetic pinch, plasma geometry, and surface tension of small cavities in D_2O, and external pressure on the TCB share some similar dynamics with hot fusion studies [5]. These hot fusion pinch studies that link to sonofusion are imploding wires, generating plasma sausage and kink deformations (these limit hot fusion reactors of the Tokamak type), and similarities to single event hot fusion inertial confinement, ICF, systems use similar physics. The advantage that sonofusion has over Tokamak reactors is that the collapsing TCB is a singular event lasting less than 1 acoustic cycle so z-pinch problems do not exist for the sonofusion systems. In fact this is what makes sonofusion work. Hot fusion plasma reactors are shut down by plasma sausage and kink modes and heavy Z contamination after a few milli-seconds giving sonofusion a big advantage over sustained fusion systems.

IMPLANT, CLUSTER, FUSION, AND HEAT PULSE

The jet plasma that does not implant as it is out of range of the target foil has no impact on sonofusion except on its efficiency. The path of the birth and death of the conical TCB jet plasma in D_2O away from the target follows a complex predictable path to its destruction. The deuteron packed jet plasma that is in range of the target foil does implant at a velocity around 30 k/sec. The period of implant adjusts and fuses deuterons in the cluster of implanted deuterons before coulombic forces start to disburse these transient clusters. At the very core of the cluster where no charge differential between ions exists and the squeeze from the exterior conversion process of deuterons plus electrons converts to bulky deuterium atoms, there is enough time for fusion to occur [6]. Figure 10 A shows a schematic of relative concentrations expected of species, during the implantation cluster process of deuterons and electrons and their recombination to deuterium atoms in the pre fusion time in the cluster of He^4 production. This process starts with a plasma jet implantation where electrons first plunge into the lattice and buildup a high concentration quickly followed by the deuterons. There is a partial charge separation during the implantation process that starts a series of processes connected to the jet plasma implantation and the very reactive species. The logarithmic time scale growth and decay of these species are shown in picoseconds along with the log of the relative temperature of the erupting fusion generated heat pulse which ends with ejecta erupting from the target ejecta sites.

An exothermic, 13.5 ev, growth of D at the surface of the D_x^+ cluster combining with near-by electrons squeezing the cluster is terminated with a DD fusion event near the center of the cluster. A series of conversions in the cluster of D^+ to D produces this fusion favorable environmental volume with a broad heat pulse that is overwhelmed by a fusion event occurring during the first picosecond of the implantation process. At the same time a spherical heat pulse is initiated and moves at a velocity near Mach 1 to the

target foil surface, (3) in figure 10. The relative temperature scale at the top of the graph shows the decreasing temperature with increasing heat pulse volume. It takes about a nanosecond for the heat pulse to reach the target foil surface, with its high temperature and pressure, where it bursts into the cavitating water as ejecta at 10^4 ^oK. The ejecta contain fusion products in the liquid/vapor state of the ejected foil. The contents of the heat pulse reaching and ejecting at the surface forms the ejecta site.

Figure 10 B shows the development of energies of the TCB jet plasma implant into a target foil. The sorting out of energies by foil examination of ejecta sites using SEM photos [9,15,16] indicates energetic processes occurring in target foils following jet impacts. A time scale in pico seconds shows the sequence of events and the energies involved at the time of implantation. Implantation of the plasma jet is about 4.5×10^{-7} Joules followed by $D^+ + e^- \rightarrow D$ conversions (2.16×10^{-18} Joules per conversion) and squeezing of the clustered deuterons. A DD fusion event occurs after about a pico second (3.2×10^{-12} Joules for one event) which initiates a nuclear heat pulse and ejects the heat pulse's contents, after reaching the target surface, into cavitating D_2O. Multi fusion events produce 3.2×10^{-7} Joules for 10^5 DD events per ejecta site.[17]

It has been a recurring thought that the clusters could have some of the properties of a BEC , Bose Einstein Condensate, being made up of deuteron Bosons with a spin of one except that the temperatures are high, but it is speculated the picosecond time frame will allow it. The white dwarf star, WDS, of very high temperatures and densities is prevented from complete gravitational collapse due to the high population of fermions (p, n, e-, ---) all with spins of half integers. It is because of the Pauli Exclusion Principal, PEP, that they, fermions, occupy space with no overlap. It is also because of this property that gravitational forces do not collapse the WDS to still higher densities. With no fuel it takes billions of years for the WDS to drop to ½ its original temperature. The Bosons particles that make up the some of the WDS contents do not conform to the PEP and will occupy less space in an over-lapping wave configuration like the BEC with their integer spins (photons, phonons, D, ^4He ---). The WDS collapse would be much greater without its fermion population. Applying this idea to the transient cluster deuteron population in the target foil in the same way it applies to WDS. The implanted clustered deuterons, makes the deuteron cluster concept of coherent Boson overlap more attractive in the context of sonofusion. Also consider this; transient coherence is understood as an extension that one finds in the characteristics of a BEC assembly - coherence of deuteron Bosons. And a possibility exists that deuterons in dense clusters may behave like electrons at low temperatures forming Cooper pair Bosons that coalesce into a liquid. A parallel to a deuteron system with those of electrons is that the D_x^+ boson clusters at higher temperature and shorter lifetimes might prolong the clusters life in the target foil. The deuteron density must have enough contact time for two core deuterons of the cluster to fuse. See figure 10A, of changes in species during implant [18].

HEAT PULSE and EJECTA SITES

The ultrasound driven piezos generate acoustic waves that pass through the D_2O producing TCBs close to target foils. Each TCB is an independent system producing transient high energy densities in the collapsing bubbles and it uniquely transfers its contents to jet plasmas of the same energy density. As the jet plasma leaves the remnants

of the TCB, the Mach 20 sheath electrons of the initial jet plasma set up a pinching magnetic field that compresses the contents to an even higher plasma density. Each jet formed is an individual deuteron accelerator. The deuteron jet implantation into the lattice of the target foils at velocities near 30 K/sec forms transient deuteron clusters in the target lattice. These clusters initially are composed of the core deuterons where DD fusion events occur and peripheral cluster deuterons that attract electrons and combine. These are chemical combinations that surround the cluster core with an inward pressure. The heat pulses accompanying the DD fusion and combination events produce two very different heat pulses with regard to amplitude and period. One, the high amplitude and short nuclear spherical expanding heat pulse for DD fusion starts in the cluster core. Two, the low amplitude and comparatively long in duration heat pulse localized in the periphery of the cluster is the deuteron electron combination to deuterium atoms. The time frame for the DD events within the deuteron cluster, after a core oscillation of D^+ in the cluster, a fusion event occurs in the order of 10^{-21} seconds initiating a nuclear heat pulse. While this is occurring the D_x^+ cluster exterior ions react with the coulombic driven electrons to form deuterium atoms initiating a chemical heat pulse that is long compared to the fusion pulse with a period in the order of 10^{-13} seconds. At time of the fusion event the cluster coherence is broken and the fusion environment destroyed. The DD events that produce ^{4}He are the origin of the nuclear heat pulses and ejecta sites.

The chemical heat pulse may exist for a few atomic oscillations with no immediate break-up danger to the core of the deuteron cluster. In fact the deuterium atoms may help to stabilize the core deuterons by forming a rapidly growing spherical outer layer around the cluster. (Normally deuterons are not stable in a Pd lattice but these rapidly forming atoms will need time to diffuse into the lattice before giving up their electron losing 13.6 ev to the target lattice.) The distribution of heat pulses with chemical origins will be easily absorbed into the target lattice and will not erupt into an ejecta site in the target foil. On this basis the ejecta sites are credited to nuclear origins rather than chemical. This was particularly evident in the 40 KHz experiments. Impulse time and relative energy of the initiation of the sharp DD nuclear heat pulse in ev/sec is 7 orders of magnitude larger than that of the chemical heat pulse. The nuclear explanation fits the observed SEM data that shows that the association energy required to produce vent sites correlates to the energy released during DD events (This was first pointed out in the proceedings of ICCF8.)

The jet plasma implant draws from a particular size bubble in the D_2O for its TCB population and therefore, all TCBs have about the same final impact energy at the time of implant. From calculations this impact energy is about $4x10^{-7}$ J –peak at 3500 nanometers. The frequency of a particular ejecta site size occurring via a size count analysis of SEM photos of Pd target foils is shown in the curve of number of sites vs their diameter. This is a typical section of a cavitation exposed Pd target foil surface 96μm^2 in area. The curve in the figure has a maximum around 200nm for an ejection site diameter. The energies in Mev or Joules can be related to the volume and diameter of the ejecta expelled via the fusion heat pulse with the number of DD fusion events occurring with each implantation into Pd target foils. Figure 11 shows the occurrence frequency of a particular site diameter that relates to a particular number of DD fusion events. In the

upper right is a schematic cutaway view showing the result of a heat pulse and ejecta breaking the surface of a Pd target foil. The site of the fusion event and the diameter of this site indicate how the ejecta energies were calculated [6]. The mass of ejecta depends on the number of DD events occurring in that target foil implant. From one DD fusion event expect to see about 24 Mev for one atom of ^{4}He produced, and about 48 Mev for two atoms of ^{4}He produced and so on. The log of the energy in joules in the bottom of figure 11 are a comparison of the two types of heat pulses 1) recombination of a deuteron with an electron (blue) and the fusion of two deuterons to form ^{4}He (red). The heat pulse blue is in the femto second range and broad compared to the heat pulse red in the 10^{-22} second range. The initial heat pulses combine and move through the target lattice at the velocity of the associated shock waves. The DD fusion impulse is much sharper.

Most of the SEM photos were of metal 100 μm thick target foils exposed to 40KHz are unique and show metal damage in the form of spheres a μm or less in diameter [19]. Also, a pattern shows an imprint of a standing induced wave of 2.6 MHz. This is why a study of sonofusion in the MHz range was undertaken. The SEM analyses of target foils show near surface damage in the form of holes, vent sites, with diameters ranging from 75 to 10,000 nanometers. The 75 nanometer vent sites convert to roughly 20 Mev events or one DD fusion event. These vent sites result from very high energy events in the lattice that release a radially growing heat pulse from the event. The heat pulses travel through the lattice to the surface as spherical waves and erupt, discharging the molten or gaseous target foil, into the cavitating D_2O. The situation regarding the typical vent site and whether the energy released is chemical or nuclear can be examined. The chemical energy of an electron combining with a deuteron is 13.6 ev and the energy for two deuterons fusing is $24x10^6$ ev. In the ICCF8 Proceedings pp 302 is a description of a single DD fusion event and the expected energy required to expel that volume of ejecta from the target foil is calculated. This is an appealing support for this heat pulse to originate from a DD fusion event. It is apparent that a million fold energy difference exists between the chemical and nuclear energy involved in the above events. It would take a million $D^+ + e^- \rightarrow D$ events occurring simultaneously to generate the same size heat pulse as one DD fusion event.

DENSITY & FUSION

When examining sonofusion and what is naturally involved it interesting to compare the environment to muon fusion where the D_2^+ molecular ion captures a muon to produce ^{3}He and a neutron at liquid deuterium temperatures. The two deuterons bonded together with the close separation allows for their fusion. There are no other close deuteron neighbors; only those two deuterium atoms with a separation 1/207 the usual bond distance, 0.105 nm in D_2 as the result of the substitution of a muon for an electron [2]. On the other hand, in sonofusion the deuterons are in the transient high density cluster with many deuteron neighbors in a coherent resonating system that allows the product ^{4}He and the excess energy to be released as a heat pulse. The transfer of energy between the locale of DD fusion and its multitude of surrounding deuterons in the D_x^+ cluster removes the energy to its surroundings as heat before a gamma can be formed.

During sonofusion, deuterons of high density produced from the TCB collapse are transferred to a pinched jet plasma, which will further increase the jet plasmas density. The high density jet plasma is implanted into the target lattice. The target lattice; for example, Pd during the implantation process, is impacted much like a micro-meteor with some differences [17]. The high density plasma implants the lattice where the large ions of argon and oxygen are blocked by the high Z lattice. The lattice bonds of the Pd atoms are broken during the impact and the Pd will be in a transient vapor state in the locale of the implant. The electrons penetrate deeper into the target lattice than the deuterons and this produces a transient charge separation and strong coulombic attraction between the two separated species in the Pd target. The deuterons at the periphery cluster interact with the mobile electrons. There is no immediate external charge effect in the core of the deuteron cluster as all deuterons are equally repulsed. Also there is a tendency of deuterons to move to the cluster surface but this is difficult with the coherence with the various attractive forces described earlier. Electrons being more mobile are moving to the deuterons where the recombination to form deuterium atoms occurs releasing the heat of formation of 13.6 ev/atom at the periphery of the D_x^+ cluster. Two points should be made. One, these recombinations occur rapidly with the exterior deuterium atoms pushing with inward force with a heat pulse ($D^+ + e^- \rightarrow D$) its heat of formation directed towards the center of the deuterium cluster and helps to counter the columbic repulsion. A transient growing spherical shield of deuterium atoms surrounds the core deuterons. Two, a short term coherence of picosecond duration delays the columbic destruction of the deuteron implant D_x^+ cluster. See figure 10.

The relative densities and therefore the D-D average separation are shown in figure 12. Some systems having environments that support DD fusion are shown to place sonofusion in a relationship to other systems with regard to their densities. The figure shows the various fusion systems (The densities are in terms of deuterons and may not be real systems.) and their expected deuteron densities vs deuteron separations (which is like plotting x vs $x^{-1/3}$). It is of interest how various fusion systems relate in their relative densities and helps to put sonofusion into a more acceptable context. The code "T" is the Tokamak systems where the deuteron density is low, 10^{21}D+/m^3. The operating temperature is in the order of 10^7 ^oK. Fusion does occur, but in a fraction of a second contamination with high Z ions and along with a z-pinch the system is shut down. "D2" is molecular deuterium with a very low probability of fusion under normal conditions, but the same configuration as muon DDμ. It fuses readily at 30 ^oK and it appears that the fusion can be explained by the increased density of the muon system. There may be a connection between the Boson character of DDμ and its easy fusion. "SUN" is the density of D^+ in the core of the Sun, noting that D^+ is controlled by the slow fusion rate of PP $\rightarrow$ D reaction in the Sun and D + P $\rightarrow$ ^{3}He + γ rate is fast, that controls the density of D^+ in the Sun's particle content. "SF" is the probable sonofusion D^+ density in the jet plasma at its implant point into the high Z targets that produce Qx heat via DD fusion. "WD" is the density and separation of deuterons in white dwarf stars if D^+ where its contents are considered as D^+ for the purpose of the figure. "Dμ" produces muon fusion in a deuterium molecular ion. The rate of muon fusion improves with lower temperatures. The size of a WD star would be much smaller if were not for the presence of fermions with their ½ spins and the Pauli Exclusion Principal. These phenomena are

especially observable in high density systems. "NS" is the density of a neutron star made up of just deuterons. "CP" is an imaginary close packed system of deuterons. "BH" is a black hole made up of deuterons or deuteron parts and a deuteron environment inside the BH horizon line where neither deuterons nor helium ions exist; only their parts do.

A COMPARISON BETWEEN SONOFUSION AND ELECTROCHEMICAL "CF".
Bubbles may be an important factor in the Fleishmann and Pons electrochemical approach to "CF". The DC electrode currents needed to produce the excess heat in the Pd electrode in electrochemical experiments can produce high frequency stress vibrations in the electrodes of an ultrasonic nature that originate as mechanical resonating bulk and surface waves much like the waves in a piezo driven system. These ultrasonic waves in the D_2O electrolyte will, if the amplitude is large enough, generate bubbles and form TCBs analogous to sonofusion. The electrode mass and geometry will modify over time to produce a bubble forming resonance within the electrode with erosion and dendrite growth on the ever changing surface of the electrode. Phenomena of this nature would account for some of the long initiation times and non reproducibility encountered. The bubbles that are generated may be from electrode frequencies in the MHz range or lower frequencies of 20 and 40 KHz with a production of frequencies other than the driving frequency like the resonance that produced the 2.4 MHz waves in the Ti target foils with a 40KHz input. [20]

Or perhaps the ripple (60,120, or higher frequencies) on the DC input to the electrode is enough to generate bubbles that collapse onto the electrode surface.

Or perhaps bubbles from the electrolytic process itself in the form of D_2 or O_2 gas bubbles are subjected to pressure gradients at the surface of an electrode. Certain size bubbles subjected to acoustic or pressure fields will rapidly collapse as in the sonofusion systems.

SUMMARY
One should differentiate between two types of fusion events; sustained events and one time events. Sustained fusion found in stars and hot fusion reactors of magnetically contained plasma (to date these have not been successful) are continuous sources of fusion power. The one time fusion event is a start and finish of a fusion event such as sonofusion, fusion bombs, inertial confinement fusion, and systems that self-destruct as they produce fusion events. At this point sonofusion is a self destructive system where TCBs and their jets produce one time fusion events as the jet plasma implants into a target foil. A hundred trillion of the controlled sonofusion jet plasma system events (10^{14} micro fusion events per second) according the DOE (Department of Energy) analysis for ^4He were found in the sonofusion product gases (554 ppm or $1.2x10^{18}$ atoms of ^4He in 19 hours of D_2O cavitation).

This summary is an attempt to look at a path that incorporates most of the experimental results over the years (called micro fusion, bubble fusion, and sonofusion) into a reasonable extension of what today is called sonofusion. The technology of

sonoluminescense, ICF , muon fusion (DDμ), MHD and electro-magnetic sonofusion jets, fiber initiated z-pinch implosions, imploding wire with a flow of electrons producing magnetic fields strong enough the turn wires to dust are related technologies that are helpful to understanding the jet plasma of sonofusion. Frozen D_2 and DT fibers in z pinch experiments with 100 to 25 μm diameter ranges are three orders of magnitude higher compared to 1.6 MHz sonofusion jet plasmas [21]. The z-pinch is a developing technology which is funded by many governments around the world. I added some ideas from this research to my development of sonofusion technologies to arrive at a reasonable DD fusion explanation for sonofusion.

The 1.6 MHz Qx production experiments are outlined here. The input energy was moderate (30 to 40 watts Qi partitioned to around 10 watts Qa) to produce the TCBs via the 1.6 MHz piezo in D_2O and implant D^+ into the target lattice via the TCB's jet plasma. It is at the end of this sequence of events. DD fusion takes place in the implanted D_x^+ cluster in the target foil that is no longer in the crystalline state but locally the target lattice is in a transient vapor state. The ejecta sites observed by SEM are too large for jet impacts with the targets. The ejecta sites formed in the cavitating D_2O submerged target foils can be correlated to energies required for 1 or more 20 Mev DD fusion events at an average rate of 10^{14}/sec. The helium four produced by sonofusion was measured in earlier experiments. One of the most difficult hurdles to navigate is the lack of the 24 Mev hot fusion gamma radiation. There are several theories that can explain our lack of gamma detection. Answers may well rest in the transient very high densities that exist in the D_x^+ created by the jet plasma implant that distribute the fusion heat to the coherent D_x^+ before a gamma photon can be formed. This high density environment in both the jet as it implants and the target lattice as it receives the deuteron plasma at a velocity of $3x10^4$ m/sec is the key. The coherent cluster of deuterons residing in the target are organized coherently and favorably so one or more fusion events will occur. The high density of 10^{33} D^+/m^3 and low temperatures of 10^4 ^oK provide for a more favorable path for the removal of energy as heat rather than a gamma. This is different than muon fusion where the density is limited to the molecule.

Results from 1.6 MHz experiments show that increasing the frequency 40 fold makes for a more efficient, economic, and usable device while still maintaining a similar Qx output. (A maximum of 38 watts of Qx from 1.6 MHz and compares with 65 watts of Qx from 20 KHz that is associated with 552 ppm ^{4}He.) The monitoring of SL is a useful tool in the determination of conditions of D_2O in the sonofusion device during the run. The relative count of SL photons/sec relates to the state of the jet plasma close to the time of its implantation into the target foil. SL occurs at the time of transfer of plasma to the high density jet plasma. Many experiments were done without foil targets indicating the similar PMT (photomultiplier) SL results for both frequency systems with and without target foils. [16]

Neutrons and long range radiation are not found as the result of measurements during and after sonofusion experiments. These results which are associated with the requirements for aneutronic fusion products ^{4}He and T are considered. As the fusion products are ^{4}He

and T is there an aneutronic path that fit the data? The nuclear paths below deliver the traditional products.

(1) $2p+2D \rightarrow 2\ ^3He+2\gamma$ 11.0 Mev
(2) $2\ ^3He \rightarrow\ ^4He+2p$ 12.8 Mev

(3) $2D \rightarrow\ ^4He+\gamma$ 23.8 Mev
(4) $2D \rightarrow T+p$ 4.0 Mev

The above paths are possibilities of known aneutronic fusion reactions that produce the products observed. There are some obvious problems; gammas are produced during measurements in the above equations (1) and (3) are not observed, but we have an explanation in the coherent high density of the D_x^+ cluster. The T product found in a Ti target experiment, equation (4), produces heat and no gammas plus T and p where the T was measured with time as the increase of the decay product ^3He associated with the T disintegration constant. This was a good fit to the analysis data [7]. The unique fusion environment of high density coherent deuterons in different high Z lattices may produce heat instead of gamma production and the low temperature of the cluster promotes (4) over its neutron producing ^3He path. When (1) and (2) are added together they produce 23.8 Mev which is the same Mev output as (3). I am sure there are paths that will fit the product data but we do not know them yet.

^4He and T, the products via the sonofusion process, produced in a unique transient environment in the target foil after an implantation of a super-dense D_x^+ cluster have been observed via our analysis. The fusion energy is removed as heat in a heat pulse rather than gamma or neutron radiation. This process presents safe and attractive alternate energy system.

What does the immediate future hold for sonofusion? The important measurements that can be made on already exposed 1.6 MHz foils that are from earlier experiments and other historically exposed foils are in storage should be analyzed by SEM and related analysis. Also, looking for more He in the exposed target lattice and T in exposed D_2O could yield interesting supporting results. There will be these and other analyses of future experiments as well as the analyses of the gases over and in the static or circulating D_2O experiments when funding or other arrangements are made.

One of the remarkable aspects of this sonofusion technology dvelopment is the application of so much of the technology that originates in hot fusion research and applies to the containment of the D^+ plasma in the sonofusion jet plasma. The sausage or kink problems in the plasma have been studied in depth and appear a milli second after the plasma initiation in relatively large plasma systems. The attempts for the various hot fusion systems to control the plasma with MHD and electric and magnetic field applications to extend the plasma's useful life has, to date, failed. What was hoped to be the continuous circulating hot fusion plasma was to be the answer for the world's growing energy problem. These results have been a major disappointment for the hot fusion community. Extrapolation of hot fusion pinch and imploding wire technology to

sonofusion has been very helpful in explaining the sonofusion process and the forces that hold and compress the jet plasma for its target implantation. The jet plasma built along the lines of a plasma capacitor with sheath electrons at the exterior and interior of the jet plasma with a velocity in the Mach 20 range have both electronic and magnetic fields that contribute to the z- pinch.

ADVANTAGES (TCB initiated sonofusion and Hot Fusion technology)

- In a fraction of an acoustic cycle millions of high velocity jet plasmas are produced.
- The z pinch collapse enhances the jet plasma's implant energy for fusion ignition.
- The imploding wire technology is parallel to the high density low energy plasma jet
- The imploding D_2 fiber technology is parallel to the high density low energy plasma jet
- The cost and size of the device is small and many units can be ganged together for larger power systems.
- A high density plasma environment is created where the fusion reaction path produces no neutrons or gammas.
- There is no worry about poisoning the D^+ jet plasma with heavy ions with the sonofusion nano-second lifetime plasma.
- The TCB collapse and jet plasma pinch system is a one time event. This micro event has a nano-second life and its remnants will be used in the next generation of TCBs.
- The jet plasma TCB accelerator,90 nm long and 6 nm in diam, implants the target foil at velocities over 30 k/sec.
- The scale and densities are extrapolated from hot fusion technology.

REFERENCES

[1] There have been over 17 years many developments in the sonofusion technology. I suggest that if one is interested they go the LENR web page managed by Jed Rothwell

[2] W. Alvarez, et al, Catalysis Nuclear Reactions by m Mesons, *Phys. Rev.*;105 1127 (1957).

[3] R. Stringham, *ICCF-7 Proceedings*, Vancouver Trade Center, Vancouver, British Columibia. Canada, ENECO,Inc., Poster #1, page #1 (1998).

[4] M. S. Plesset, and R. B. Chapman, *J. Fluid Mech*.,47, 283 (1971)

[5] M. A. Liberman, J. S. De Groot, A. Toor, R. B. Spielman; *Physics of High-Density Z-Pinch Plasmas*;Springer, QC718.5.P45P48, (1998) & T. C. Kausuik, N. K. Gupta, and S. H. K. Auluck, Bhabha Atomic Research Center, Trombay,Mumbai-400 085 (India).PDF

[6] R. Stringham, *ICCF-10 Proceedings*, Poster, Boston, MA, USA, Aug (2003

[7] Brian Oliver; DOE MS analysis of 4He & 3He for EQuest Sciences, reported in Roger Stringham, *APS Proceedings*, Seattle, WA. (2001) & APS 2001
R. Stringham, *ICCF-8 Proceedings*, Villa Marigola, LaSpezia, Italy,299-304, May (2000)

[8] R. Stringham, *ICCF-8 Proceedings*, Villa Marigola, LaSpezia, Italy,299-304, May (2000) & R. Stringham, *APS Proceedings*, Baltimore MD, Mar. (2006)

[9] R. Stringham, *ICCF-8 Proceedings*, Villa Marigola, LaSpezia, Italy,299-304, May (2000) & Roger Stringham, *APS Meeting, Seattle*, WA, video (2001)

[10] R. Stringham, *ICCF-10 Proceedings*, Poster, Boston, MA, USA, Aug (2003) & R. A. Heller and S. J. Putterman, *Phys Rev. Lett*., vol 75,No.19, 3549, (1995).

[11] R. Stringham, ICCF-11 *Proceedings, Marseilles*, France, page 238, Oct. (2004) & DVD

[12] S. Chubb, *ICCF-11 Proceedings*, Marseilles, France, 646, (2004) & Y. Kim and A. L. Zubarev, ICCF-8 Proceedings, Villa Marigola, LaSpezia, Italy,375-384, May (2000) & P.L. Hagelstein, *ICCF 8 Proceedings*, International Convention Center, Tsinghua University, Beijing, China,121, May (2002)

[13] K. R. Weninger, P. G. Evens, and S. J. Putterman, *Phys. Rev. E.* **61**(2), 3 (2000)

[14] Y.Tomita, A. Shima; *Acoustica*, 71,161 (1990) and M. P. Felix, A. T. Ellis, Appl. Phys. Lett. 19, 484, (1971) and W. Lautterborn, H. Bolle, *J. Fluid Mech*., 72,391 91975).

[15] R. Stringham, *ICCF-8 Proceedings*, Villa Marigola, LaSpezia, Italy,299-304, May (2000)

[16] Many SEM unpublished cavitation exposed target foils photos the effects of this consistant type of damage.

[17] R. Stringham, *APS Proceedings*, Baltimore MD, figure 7 Mar. (2006)

[18] R. Stringham, APS Proceedings, Baltimore MD, figure 6A Mar. (2006) & R. Stringham, *APS Proceedings*, Baltimore MD, figure 7 Mar. (2006).

[19] R. Stringham, *ICCF-8 Proceedings*, Villa Marigola, LaSpezia, Italy,299-304, May (2000)

[20] R. Stringham, *ICCF-7 Proceedings*, Vancouver Trade Center, Vancouver,British Columibia. Canada, ENECO,Inc., Poster #1, page 16 (1998).

[21] M. A. Liberman, J. S. De Groot, A. Toor, R. B. Spielman; *Physics of High-Density Z-Pinch Plasmas*;Springer, QC718.5.P45P48, page 238-241 (1998)

Fig. 1

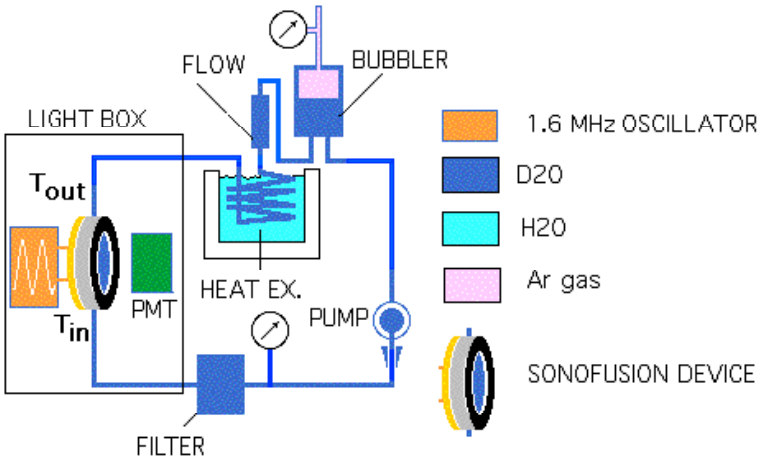

Figure 1. The experimental sonofusion system was set-up to measure the temperature difference between the input and output. The two measurements Tout – Tin = ΔTss, and the D_2O flow are the two parameters describing the calorimetry. D2O flow x ΔTss x 4.184 measurement are the Qo watts output from the device. The system consists of the following components. The 1.6 MHz piezo oscillator device, orange rectangle with sine-wave, drives the piezo of the Series 1 A sonofusion device, as the D_2O, blue, is circulated through the device at a constant rate by the mass flow FMI pump. The D_2O is saturated with Ar in the bubbler, pink and blue. In the circulation line are the pump, filter, sonofusion device, heat-exchanger flow-meter, and bubbler in that order. The heat-exchanger's H_2O, light-blue, removes heat from D_2O maintaining a constant temperature in the sonofusion device as the D_2O circulates. The PMT, photomultiplier device, green, measures the level of SL photons that indicate the condition of the plasma in the final stage of the TCB collapse. These experiments required complete darkness and were done in a light box (no outside light interference) with circulating air maintaining a constant running temperature during experiments. The parameters that control SL are the temperature of the D_2O, the pressure of Ar over the D_2O, and the acoustic input from the 1.6 MHz oscillator.

In the D_2O flow line was a sintered stainless steel 20μ particle filter that kept the sonofusion device circulation system free from debris blockages. The bubbler was connected to a vacuum gas handling system that kept the pressure at one atmosphere of Ar. The 20 gm mass made up of the 3.5 gram piezo (heat capacity, C, of 0.8 J/gm) and 16 grams of plastic (heat capacity of 1.7 J/gm and 1gm of D_2O (C of 4.0 J/gm) gave a C for the 20 gm device of 1.7 J/gm.

The heat capacities, C, of the materials used in the construction of the sonofusion reactor were 1.7 J/gm for plastics and a 0.8 J/gm 1.6 MHz piezo for glass.

For example Run, Series 1 A Run # 6, with small convection losses, Q(convection loss) =0.04 watts, (calculated from the convection loss graph, ΔTss vs Qa + Qx – Qc and had a Qa of 16.6 watts (the input to the sonofusion D_2O) The sum of all the heat out of the reactor, Qo=(Qa+Qx-Qc), of 54.8 watts and a ΔTss of 14.3 ^{o}C produces an excess heat of 38.2 watts. The Qc is small in these experiments and can be ignored.

Fig. 2

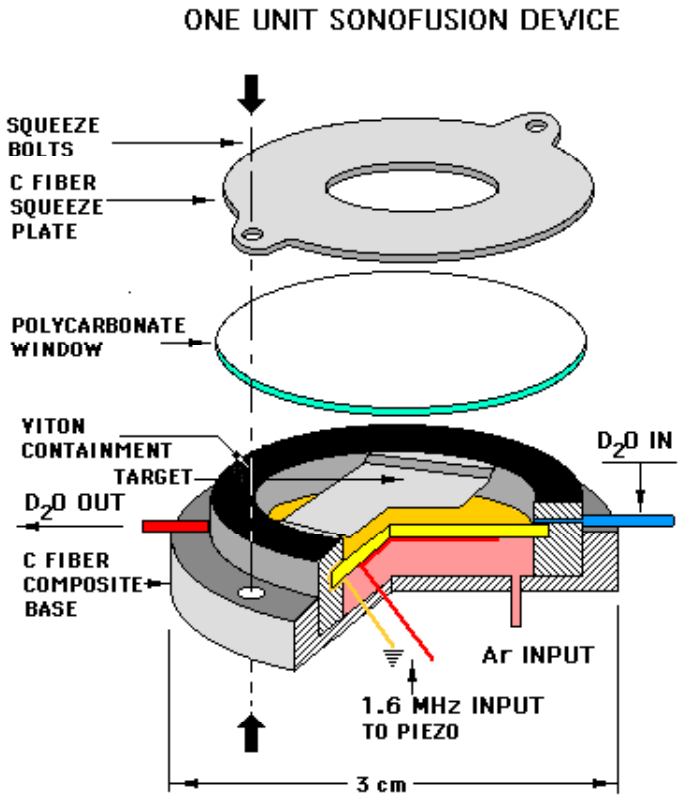

Figure 2 is a schematic of a one unit sonofusion device showing its 20 gm use of materials and its geometry. The physical orientation of the running device would usually be rotated 90°, with the window perpendicular to the earth's surface with the input at the bottom. The general configuration is concentric elements that are squeezed together with nylon bolts forming a water-tight reaction chamber for the circulating cavitating D_2O. The piezo is clamped by the same squeeze as the target foil. The D_2O inputs and outputs are arranged so that there is a pulsing pressure in the cavitating D_2O that originates from the FMI circulating pump in the 1 cc reaction volume. Ar pressurization of the space under the piezo is for higher pressure runs and has been used on occasion. The two electric leads are from the 1.6 MHz oscillator and they power the piezo that is the acoustic input, Qa. The carbon fiber composite base provides a seal for the Ar and base for the squeeze that makes the device water-tight. The Neoprene containment and holder for the 1.6 MHz piezo is the main sealer for the D_2O and Ar containment. The 40 mil polycarbonate window finishes the seal for the reaction volume. The carbon fiber squeeze plate with a hole for a PMT window allows for the count of SL photons. The concentric elements are held in place by two nylon bolts that provide the squeeze and seal for the sonofusion device via the base plate. With the squeeze in place the target foil is held tightly and acts as a shield for the window, blocking most of the cavitation activity from damaging the SL window.

Fig. 3

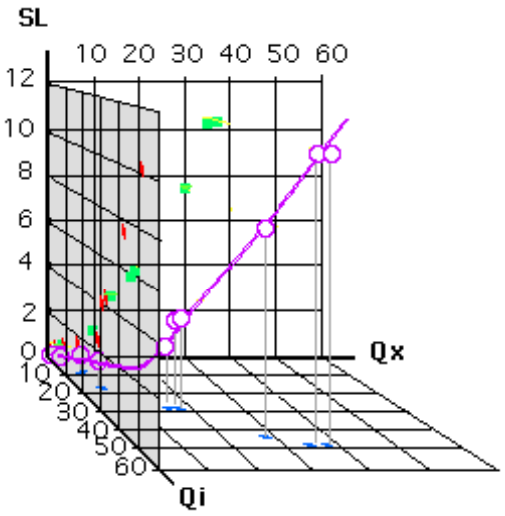

Graph of Series 1 A Data

Fig. 4 Table

Watts Excess Qx	Watts in (wall) Qi	K counts/ sec. PMT SL
14.5	29.0	2.7
18.3	29.4	4.2
16.4	29.4	4.4
28.6	43.4	7.5
34.3	50.4	10.5
38.2	50.4	10.5
7.5	17.0	1.1
4.0	9.4	0.7
1.3	4.2	0.1
0.6	2.0	0.0

Table of Series 1 A Data

Graph 3 shows the resultant, purple, of the data, from the low mass (20 gm) 1.6 MHz sonofusion device, collected for the three parameters (Qx, Qi, and SL) measured during the experiments of Series A. SL, sonoluminescence, indicates the presence of the high density partial plasma from the collapse of TCBs in D_2O. The TCB collapse process produces jets during the last stage of the bubble collapse. These jets contain a deuteron and electron plasma that is accelerated and implanted into a metal target where sonofusion takes place producing Qx, excess heat. The energy density and velocity of the implanting transient micro sonofusion jet is $10^{31}D+/m^3$ and 30k/sec. Qi is the 120 volt 60 cycle input from the wall which is related to Qa, the 1.6 MHz piezo acoustic input (Qa = 0.33Qi). The Qx = Qo-Qa, where Qo is the measurement of the total heat out. The error on these measurements is about + or – 5 %.

Figure 4 The table of the data used in figure 3 is taken from the complete data table of figure 5. The three parameters are the excess heat, Qx, in watts; the input watts, Qi, from the 120V 60 cycle wall socket; and the SL photon count in 1000 photons/sec via the PMT (A background count/sec between 60 and 100). The data could have been using Qa, the acoustic input instead of Qi the total input. The SL is produced in the last phase of the TCB collapse and is important with respect to the presence of a plasma at the point the TCB collapse forms a jet. The jet plasma is the key to the fusion path that is proposed.

Fig. 5 Table

TABLE - More Complete Data Set for Series 1 A

1.6 MHz Data Pulsed & Continuous (Pd#2 Target; D2O 99%; Ar 1 Atm.)

PRELIMINARY DATA

Ar for all runs was 1 atm.

* Series C run 7 was 2 atm. - producing more photons but not more Qx

** Geiger M. counter

0	1	2	3	4	5	6	7
Date 04	duty cycle on = off	Run series A	1000 pho/sec. PMT SL	Variac input soni VOLTS	Watts in Qi	Circ. Flow ml/min	Reactor DT ºC
6 Aug.	30on-30off	1	2.7	100	29	55.00	6.3
	continuous	2	4.2	100	29.4	55.00	7.3
	30on-30off	3 CC 3	4.4	100	29.4	55.00	8.0
	30on-30off	4	7.5	130	43.4	55.00	11.2
	30on-30off	5	10.5	140	50.4	55.00	13.3
	60on-60off	6	10.5	140	50.4	55.00	14.3
	60on-60off	7	1.1	80	17	55.00	3.4
	60on-60off	8	0.7	60	9.4	55.00	1.8
	60on-60off	9	0.09	40	4.2	55.00	0.7
	60on-60off	10**	0	30	2	55.00	0.3
	60on-60off	11**	20	140	50.4	55.00	6.0

8	9	10	11	12	13	14	15
Watts out Qo	Acoustic Watts in Qa	Excess Heat out Qx	Qa+Qx-Qo	Watts over unity OU watts	Cavitating Reactor liquid	Comment Problems	MF (Qi+Qx)/Qi
24.0	9.5	14.5	0.0	-5.0	D2O	New Rx	1.50
28.0	9.7	18.3	0.0	-1.4	D2O		1.62
30.7	14.3	16.4	0.0	1.3	D2O		1.55
43.0	14.3	28.6	0.0	-0.4	D2O		1.65
51.0	16.7	34.3	0.0	0.6	D2O		1.68
54.8	16.6	38.2	0.0	4.4	D2O		1.75
13.1	5.6	7.5	0.0	-3.9	D2O		1.44
7.1	3.1	4.0	0.0	-2.3	D2O		1.42
2.7	1.4	1.3	0.0	-1.5	D2O		1.31
1.2	0.7	0.6	0.0	-0.8	D2O		1.28
23.0	16.6	6.4	0.0	-27.4	D2O	leak - overheated	1.12

Figure 5 shows a more complete set of data for Series 1 A and below are the keys to the data columns.

0 Date of run.
1 The duty cycle for pulsed SF device in seconds.
2 Run number.
3 Photomultiplier measurements of relative SL photon emission from SF device in 1000 photon PMT units.
4 The 140 to 0 volt 60 cycle variac input Qi.
5 The Qi input in watts to the SF device that produces Qa.
6 The ml/min of Ar saturated D_2O circulated through the1cc SF device.
7 The ΔTss of the in & out ports of the D_2O circulation through the SF device.
8 Qo is the total heat out (Qa + Qx) at steadystate temperature =(ΔTss*FR*4.184 watts).
9 Qa is the acoustic input from 1.6 oscillator to the SF device.
10 Qx is the excess heat produced. Qx = (Qo-Qa).
11 Data check. Qa + Qx = Qo
12 Over unity watts Qo-Qi = OU (over unity)
13 The cavitating liquid in SF device.
14 Some comments and problems about the Run.
15 The watt multiplication effect. M = (Qi + Qx)/Qi

Fig. 6

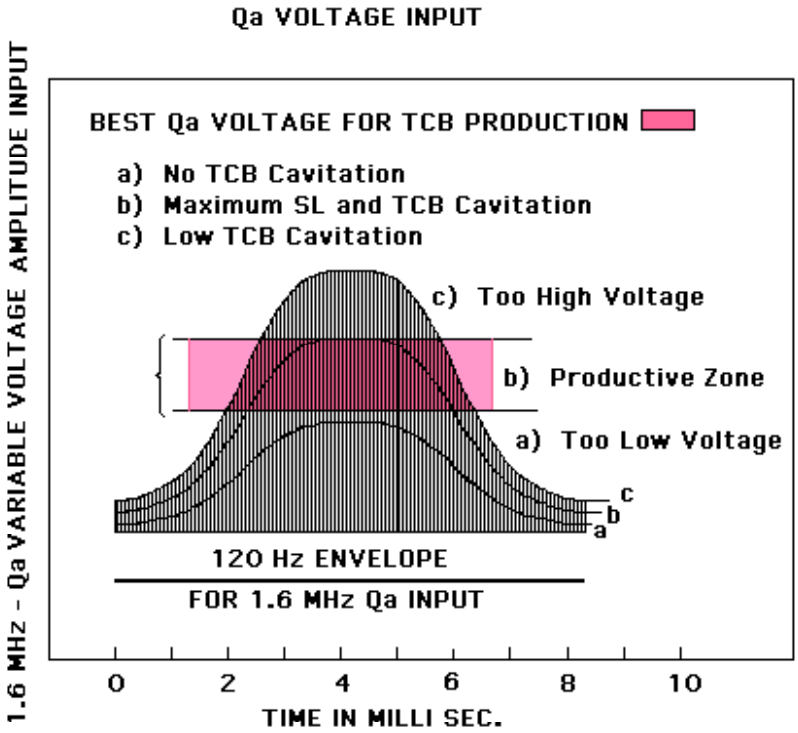

Figure 6. The production of TCBs in D_2O depends on the two parameters of D_2O temperature (vapor pressure) and of the external pressure of Ar. The 1.6 MHz oscillator supplies the power to the piezo, Qa, that cavitates the D_2O in the sonofusion device, which can be varied using a variac that controls Qi, the device input. The 1.6 MHz Qa power (amplitude) is proportional to the sinusoidal 120 Hz envelope from the oscillator that carries acoustic input to the piezo. The figure illustrates the variable voltage of the Qa amplitude input to the piezo and its effect on the TCBs. A TCB requires a particular voltage amplitude to gain its maximum energy density during its collapse process. This zone, shown in magenta, is the most effective voltage amplitude and is coupled with the temperature and external pressure of the TCB system. The resonance Qa amplitude coupled to the growth and mass of the TCB for a particular 1.6 MHz cycle should fall in the magenta zone shown in the figure. If the Qa input level is (a) there will be no TCB generation and therefore no SL. If the Qa input level is (b) close to 50% of the signal time it will produce TCBs and SL. However, if the Qi input is too high as in (c), the TCB output will be less than 10% and a lower level TCB and SL will be present. The 120 cycle input favors the production of a maximum number of TCBs and SL when the 1.6 MHz voltage amplitude is b in the magenta zone.

The acoustic signal delivered to the D_2O with the correct temperature and external pressure will produce millions TCBs/cc (volume of one million jet plasmas is $4.7*10^{-13}$ cc) in one 1.6 MHz cycle and produces the same number of accompanying jet plasmas. It is important to get the relationship between SL and the three coupled parameters 1) Qa, 2) temperature, and 3) external pressure at the correct values for the sonofusion process to produce fusion events. (The running parameters for the Series 1 A run #6 were a Qa of 16.6 watts, a pressure of 1 atmosphere of Ar, and a temperature 30 ^{o}C for D_2O with a SL count of 10,500 photons – a relative number.) This figure is for 1.6 MHz systems but applies to the 20 and 40 KHz systems.

Fig. 7.

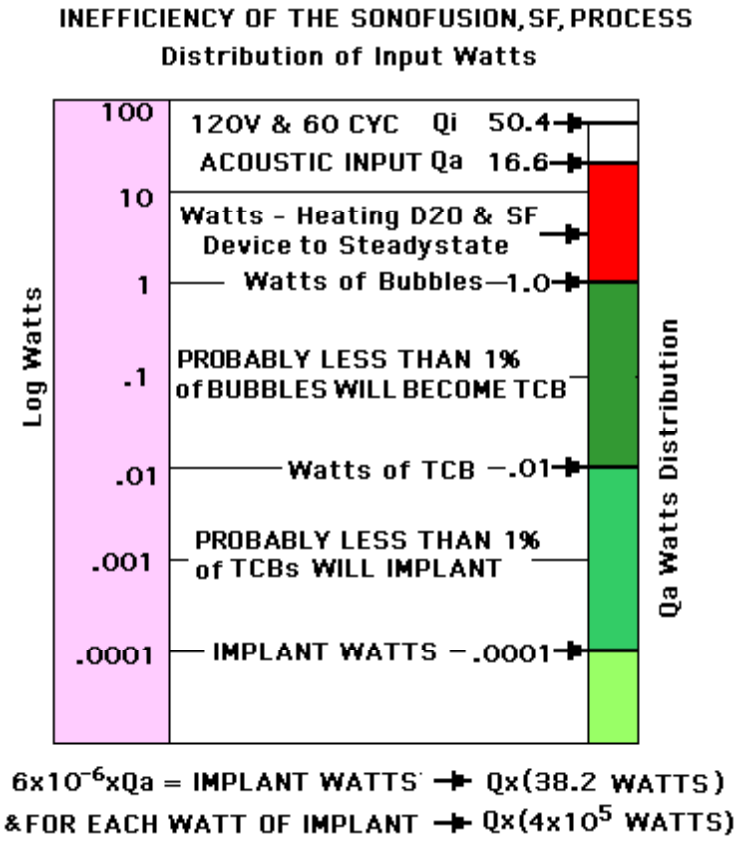

Figure 7. The efficiency of the 1.6MHz sonofusion system when producing Qx heat is quite low when the mechanics of involved factors from Qi to Qx are evaluated (Qi is the total power input and Qx is the excess heat). These factors can certainly be changed to improve the efficiency. The Series 1 A experiment where Run 6 passes from a variac Qi of 140V and 50.4 watts to produce a Qx of 38 watts of excess heat. The power to the oscillator takes 2/3 of Qi to produce a Qa (the total acoustic input) of 16.6 watts of a 1.6 MHz of acoustic input. The Qa input mostly heats the sonofusion device and circulating D_2O. Only a small amount of Qa, about a 1 watt, is used to create TCBs and jet plasmas. From the total bubble population a small portion of that population is the resonant proto-TCB population and it grows rapidly to its maximum radius in the negative pressure region of one acoustic cycle. Immediately following this maximum is a violent pseudo adiabatic bubble collapse of the TCB population that may number a percent of the total bubbles present. Of the jet plasmas that are produced something less than 1% has the potential to implant into the target foil. Of the original Qa watts only 100 micro watts or less are involved in the implantation process into the target.

To the right side of the figure is the distribution of Qa watts. It is obvious that most are used in heating the piezo, the circulating D_2O, and the SF device -shown in red. The bubble formation is shown in green. The total watts of Qa used is about 1 watt shown as dark green. This was determined by the height of a 15 cm. column of water generated in an open SF device. Of the total bubble population probably less than 1% are TCBs that are in resonance with the SF device and its piezo and this is shown as middle green. The TCBs that implant the target foil are probably less than 1% of the TCB population and shown as the light green color in the lower right hand corner. In the example, the light green TCBs that implant account for all the 38.2 watts of Qx produced. This scales to $4x10^5$ watts for one watt of TCB implants in Series 1.A, Run #6, at 1.6 MHz. This figure is for 1.6 MHz systems but applies to the 20 and 40 KHz systems.

Fig.8

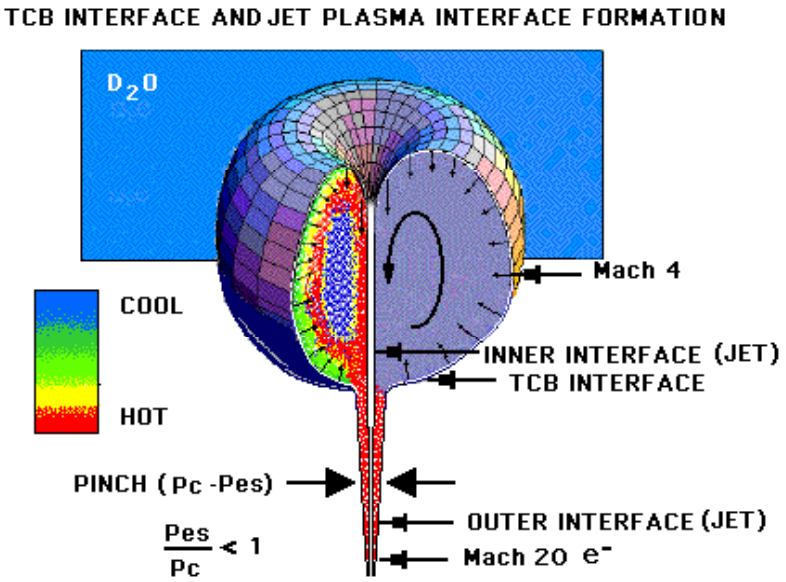

Fig. 8. This schematic figure of a TCB in its final stage shows a path to the jet plasma formation. A plasma jet is formed during the last stage of the TCB's implosive collapse. During the imploding collapse, the D_2O interface (skin) performs an amazing organizational stretch while expelling its TCB plasma contents into the jet plasma and into the circulating D_2O (The events associated with the TCB collapse are so transient that the circulating D_2O may as well be static). The interface is a very flexible surface tension linked system similar to the skin that transforms into a plasma sheath of electrons enhanced by magnetic and electric fields that separate high density jet plasma from low density D_2O. The figure illustrates the flexibility of this surface tension skin interface system in a cutaway of the last stage of the TCB collapse where the right hand side of the TCB has its contents removed to expose the collapsing interface. This interface moves to the TCB center at a velocity of Mach 4, maybe more. During this collapse, just before the final stage, the top of the collapsing TCB is pushed by the acoustic wave front and the proto-jet starts as a dimple on the TCB surface forming a jet plasma traveling at a velocity of 20 Mach that includes some of the collapsing TCB's contents (plasma) that circulates into the jet. Shortly after the jet plasma disengages from the TCB Mach 4 interface and bubble remnants, the jet plasma becomes a deuteron accelerator. Note, the collapsing volume of the TCB pumps its plasma into the jet forming a toroidal geometry for the last stage of the TCB. The jet plasma is further compressed by the z pinch ($P_{ST} + P_E + P_{JxB} - P_{es}$) as it implants into the target. The ratio of P_{es}/P_c being less than 1.0 squeezes the plasma to a compressing conical geometry. Also note that as the interface of the TCB is the phase boundary between D_2O and the gas phase initially, with the final state of the TCB contents (a density of 10^{31} D^+/m^3), this interface rapidly becomes the jet's interface boundary and now isolates the high density jet plasma from cavitating D_2O (in this time frame the D_2O is static). Cavitation of the D_2O at this point is in its positive pressure zone of the acoustic wave activity. This jet formation process also causes the jet plasma contents to move coherently as a mono-energetic plasma unit before it implants into the target. This figure is for 1.6 MHz systems but applies to the 20 and 40 KHz systems.

Fig. 9.

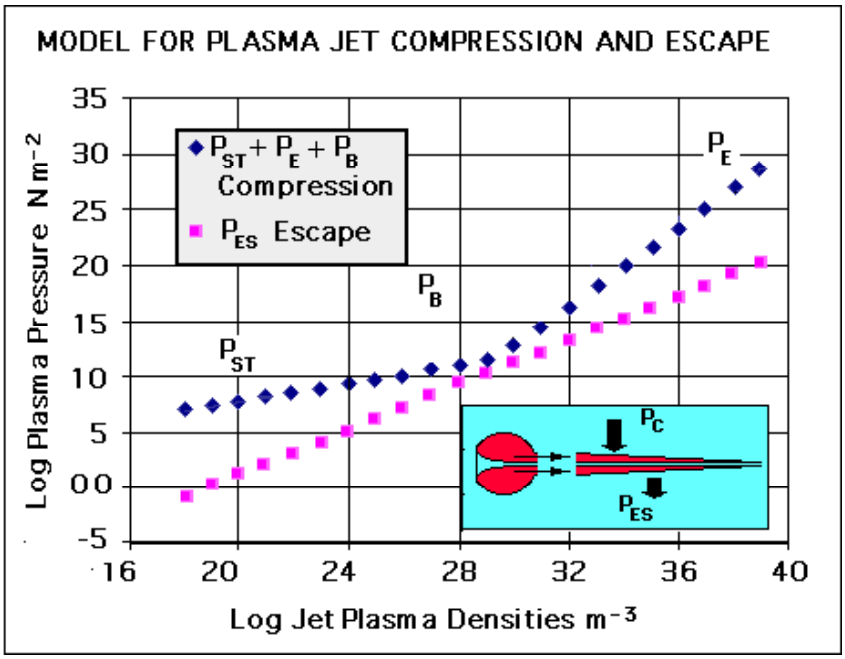

Fig, 9. The TCB plasma jet owes its conical geometry to opposing pressures generated from the high density low energy plasma contents of the jet that has velocities of over 10k/sec. For example, the plasma contents, which may initially be at a density of 10^{31}deuterons/m^3 and the same for electrons (10^{25} deuterons/cc) in the jet plasma volume will be compressed to higher densities by the compression pressure, Pc, minus the escape pressure, Pes. The z pinch is the sum of pressures ($Pc = P_{ST}+P_E + P_B$) and these are pressures from surface tension and electric and magnetic fields. Pes is the escape pressure nkT. The plasma temperature for this model is placed at 10^4 ^oK, but could be raised (magenta squares Pes and blue diamonds Pc). The jet plasma volume contents are a projectile-like plasma (a deuteron accelerator) of the TCB collapse process. The jet plasma takes the form of an elongated cone with a base radius of $3x10^{-9}$ m and a length of $90x10^{-9}$ m for the 1.6 MHz system. The graph shows the stability of the transient jets during the pinch process. The lifetime of the TCB jet plasma is very short, in the order of picoseconds. The geometry of the jet plasma is complex and adds more compression to Pc due to its hollow nature. See fig 8. The magenta squares in the figure show that the Pes increase as the D^+ density increases. The blue diamonds show Pc increase as the D^+ density squared increases at a higher rate than Pes. The graph shows that as Pc increases, it might maintain its stability to white dwarf star densities [5]. The density range goes from below that of a Tokamak (10^{21} deuterons/m^3) to that of a star. Pc increases the jet plasma compression pressure where at low densities the compression is controlled by P_{ST} pressures. As the density D^+/m^3 increases the compression pressure, the cross product of JxB converted to pressure, near the break in the Pc curve P_B is responsible for the mid range of the pinch compression. In the high densities the Pc compression takes over in the form of P_E. The P_E and P_B are calculated with the initial temperature plasma velocity, v_d, of $3*10^4$ m/sec and does not reflect the increase in temperature with the increase in pressure and decrease in volume. The TCB in its final stage is around densities of 10^{30} to 10^{31} and is the jet plasma initial density and involves about 10^7 particles. With these conditions there is a sheath current of 1 amp. ($Ns = 10^4$ sheath electrons) that produces an increasing transient compression via electric and magnetic fields in the jet plasma. These fields will rapidly increase as the jet plasma is compressed and will continue to increase until the jet plasma is pinched off or implants. This figure is for 1.6 MHz systems and is similar to the 20 and 40 KHz systems. More on the compression pressures that increase the jet plasma's implant density will be found in the Appendix.

Fig. 10 A&B

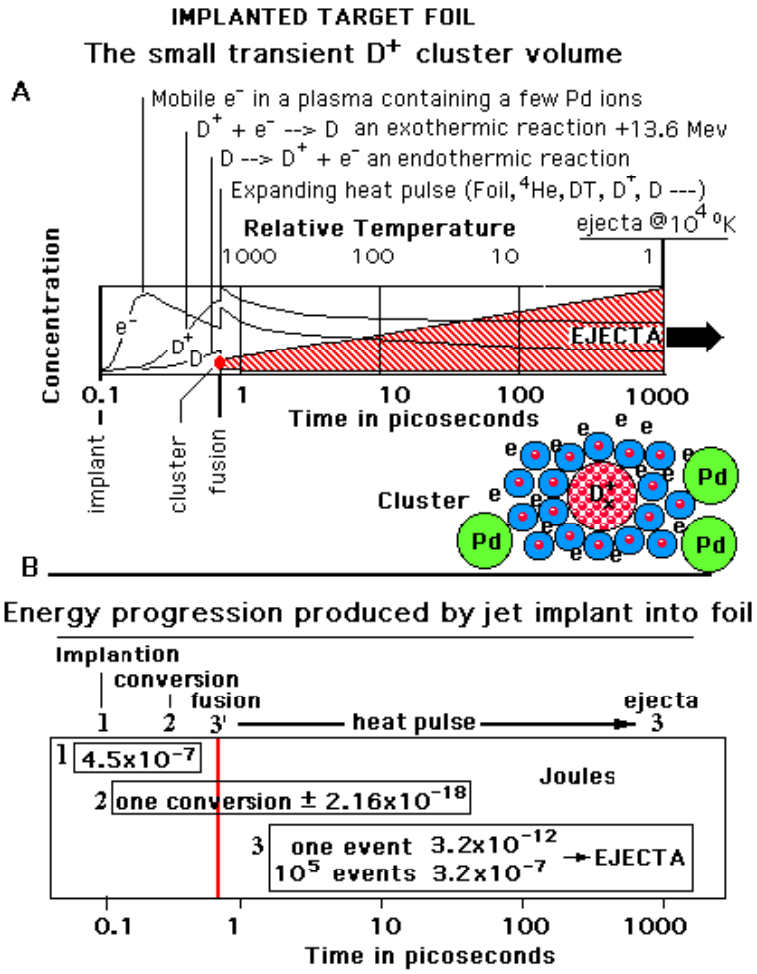

Fig. 10 A&B. In the cluster of implanted deuterons, D_x^+, as the coulombic forces start to disburse these ions in the very core of the cluster, they feel reduced charge differential in high density Bosonic deuterons. The D_x^+ is similar to an electron liquid where an electron is shielded from coulomb forces by other electrons A cluster squeeze consists of a boson wave overlap with its coherence effect and the production of deuterium (D conversion process) at the cluster surface keeps the cluster from disbursing as readily as expected via coulomb forces. These estimations are for a 40KHz system.

Figure A shows a schematic of relative concentrations of expected species during the implantation, during the period of cluster existence, timing of the fusion event, and the resulting heat pulse. This process starts with a plasma jet implantation of electrons that plunge further than the deuterons into the lattice setting up a charge separation buildup to a high concentration of mobile electrons attracted to deuterons in their cluster. The logarithmic time scale growth and decay of these species is shown in picoseconds along with the log of the relative temperature. An exothermic, 13.5 ev, growth of D at the surface of the D_x^+ (x may vary from 10^3 to 10^5 deuterons) cluster combining with nearby electrons squeezing the cluster and is terminated with a DD fusion event(s) near the center of the cluster. A series of conversions in the D_x^+ cluster to D and the deuteron boson character produce this fusion favorable environmental volume via coherence of deuteron bosons. The broad heat pulse from the D conversion process is overwhelmed by a fusion event occurring during the first picosecond of the implantation process. At this time a sharp spherical heat pulse is initiated

(3') and moves at a velocity near Mach 1 to the target foil surface (3) producing ejecta. The relative temperature scale at the top of the graph shows the decreasing temperature with increasing heat pulse volume. It takes about a nanosecond for the heat pulse to reach the foil surface, with its high temperature, 10^4 °K, and pressure, where it bursts into the cavitating water as ejecta, containing fusion products in the liquid/vapor state of the target foil.

Fig. 10B. The developed energies of the TCB jet plasma that implant into a target foil producing fusion ejecta are shown. The sorting out of energies with a survey of SEM foil photos of ejecta sites indicate energetic processes of various sizes occurring in target foils following jet impacts.

1 –Implantation events –The implant of 10^5 D^+ and D into the target foil (stripping D to D+) with a velocity of $3x10^4$ m/s produce about $3.5x10^{-7}$ Joules for each TCB implantation
2 – Conversion events - The exothermic $D^+ + e^- \rightarrow D$ (and later the endothermic $D \rightarrow D^+ + e^-$) at the implant site and cluster surface can be viewed as a heat pulse spread over the entire cluster transient life-time, about a picosecond. The 13.5 ev exothermic and endothermic ($D+ + e^- \leftarrow\rightarrow D$) process is canceled in the long term but initially may contribute to a fusion heat pulse, 3' & 3, and the transient temperature environment of reaction volume in the target foil. Only a small amount of the D conversion energy is available to use in the ejecta heat pulse at 13.5 ev per conversion event. This is a competition between deuteron conversion and bosonic squeeze (coherence) on one hand and coulomb repulsion on the other.
3' & **3** – The fusion event occurring within the D_x^+ cluster implanted in the foil, 3', releases a heat pulse, with a very sharp impulse, that will travel to the foil surface in about a nanosecond ejecting vaporized foil and its contents into the cavitating water at 3. The volume of ejecta cast into the water leaves a hole in the foil surface that is photographed via SEM analysis. The population of ejecta sites of a given size follows a distribution curve, shown in fig. 11, with energies varying from $3.2x10^{-12}$ J for one DD event and to $3.2x10^{-7}$ joules for 10^5 events per ejecta site. This figure is for 1.6 MHz systems but applies to the 20 and 40 KHz systems.

Fig 11

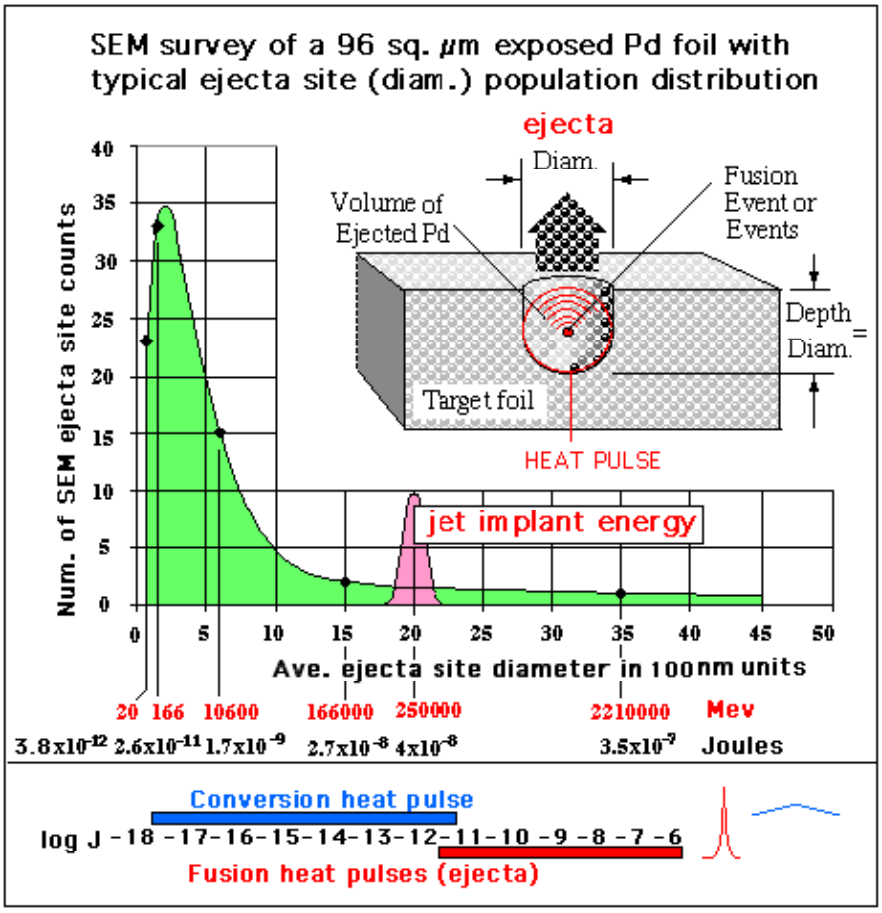

Fig. 11. The jet plasma implant draws from a particular size bubble in the D_2O for its TCB population; therefore, all TCBs have about the same final impact energy at the time of implant. This figure is for a 40 KHz system. From calculations this impact energy is about $4x10^{-7}$ J –peak at 3500 nm in magenta. The frequency of a particular ejecta site size occurring via a size count analysis of SEM photos of Pd target foils is shown in the curve of number of sites vs their diameter (in 10^2 nanometers units). This is a typical section of a cavitation exposed Pd target foil surface 96μm^2 in area in a SEM photo analysis. The curve in the figure has a maximum around 200nm for an ejection site diameter. The energies in Mev or Joules (red and black) can be related to the volume and diameter of the ejecta expelled via the fusion heat pulse with the number of DD fusion events occurring with each implantation into Pd target foils. The graph shows the occurrence frequency of a particular site diameter that relates to a particular number of DD fusion events. In the upper right is a schematic cutaway view showing the result of a heat pulse and ejecta breaking the surface of a Pd target foil. The site of the fusion event and the diameter of this site indicate how the ejecta energies were calculated. The mass of ejecta depends on the number of DD events occurring at the site in that target foil implant. From one DD fusion event expect to see about 24 Mev for one atom of ^4He produced, and about 48 Mev for two atoms of ^4He produced and so on. The 40 KHz system from which these data were gathered is applied to the heat pulse analysis at the bottom of the figure. (For a 1.6 MHz system the number of deuterons is 10^7 instead of 10^{11} as estimated for the 40 KHz system leading to much bigger sites) The log of the energy in joules in the bottom of figure is a comparison of the two types of heat pulses 1) recombination of a deuteron with an electron (blue) and the fusion of two deuterons to form ^4He (red). The heat pulse blue is in the femto second range and broad compared to the heat pulse red in the 10^{-22} second range. The initial heat pulses combine and move through the target lattice with the associated shock waves at a relatively slow velocity. The DD fusion impulse is much sharper and bigger.

Fig. 12 .

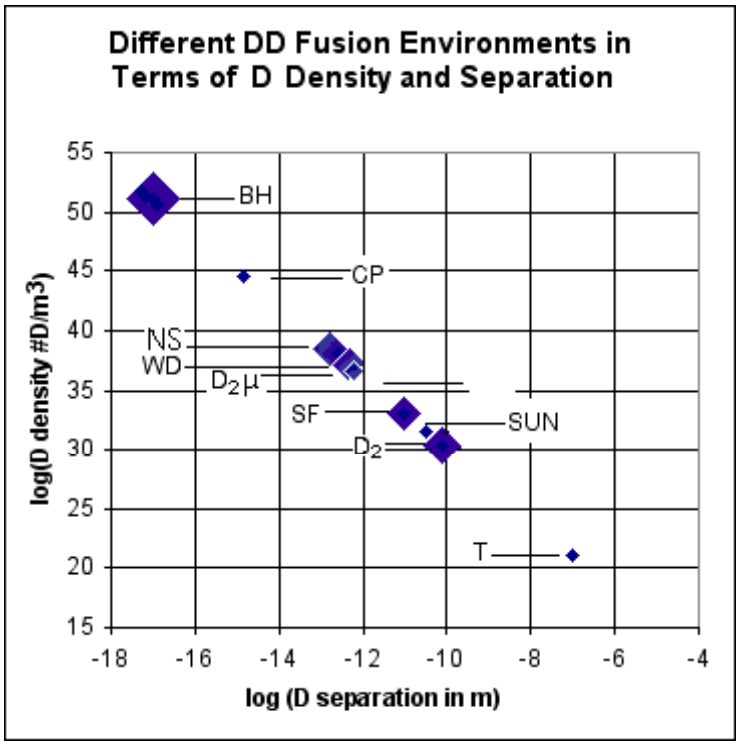

Fig. 12. The relative densities and therefore, the D-D average separation of some systems have the potential to produce DD fusion in the systems environment. We know that high densities alone can produce DD fusion, as in muon fusion that depends only on the distance of separation between two deuterons are involved. This is unique because only two deuterons produce a fusion product and is free from a temperature influence. There are two different kinds of densities, those with large numbers of deuterons as in stars, and those where just two deuterons are coupled as in muon fusion. Sonofusion in relationships to other systems with regard to their densities is more like a star system. The figure shows the various fusion systems where the densities are in terms of deuterons and may not be real systems (the basic environment is real). Their expected deuteron densities vs deuteron separations (which is like plotting x vs $x^{-1/3}$) refers only to one parameter of its fusion environment. It is of interest how densities relate and help to put sonofusion into its density context. The code "T" is the Tokamak system where the deuteron density is low, a partial vacuum at $10^{21} D^+/m^3$. The operating temperature is in the order of 10^7 ^oK. Fusion does occur during the fraction of a second before contamination with high Z ions, z-pinch, coulomb repulsion, and diffusion shuts down the implant system. "D2" is the molecular deuterium with a very low probability of fusion under normal conditions. But the same configuration as muon DDμ fusion that readily fuses at 30 ^oK and its fusion can be explained by the increased density or decreased separation of the two deuterons "SUN" is the density of D^+ in the core of the Sun, noting that D^+ is regulated by PP → D, the slow and controlling rate of fusion, and D + P → $^3He + \gamma$ a fast rate of fusion. These rates control the density of D^+ in the Sun's particle content. "SF" point on the graph is the probable sonofusion D^+ density in the jet plasma, but there are suggestions [21] that its limit is the density of a WDS. Sonofusion can improve its fusion chances relying on the Boson character of D^+_x. "D2μ" produces muon fusion in a deuterium molecular ion. The rate of muon fusion improves with lower temperatures. The separation in D2μ is 1/207 that of D_2. Muon fusion does not have the numbers of deuterons that the sonofusion D^+_x implant does in the high Z targets. "WD", sun-like stars that have collapsed to high densities and have run out of low Z fuel including deuterons are dead stars slowly losing their heat. The WD contents are deuterons just for the purpose of this figure and would certainly fuse any deuterons present. The size of a WD star would be much smaller if it were not for the presence of fermions, their ½ spins, and the Pauli Exclusion Principal that limit WD's collapse against gravity. "NS" is the density of a neutron star made up of deuterons and is an imaginary environment. "CP" is an imaginary close packed system of deuterons. "BH" is a black hole

made up of deuterons or deuteron parts on the other side of the BH horizon line where neither deuterons nor helium ions exist; only their parts do. Only the hypothetical environments exist in WD, NS, CP, and BH, and if any deuterium were present it would fuse.

APPENDIX

Sonofusion Jet (Electric & Magnetic Fields)

The magnetic field created by the velocity, v_d, of the jet's sheath electrons and the corresponding electric field from the jet slicing through the dielectric D_2O produces a pinch on the conical jet plasma's contents preventing the nkT escape of particles. This compression originates from the Lorentz Force Law, $\mathbf{F} = N_s q\mathbf{E} + N_s q(\mathbf{v}_d x \mathbf{B})$, and/or the electromagnetic, EM, Maxwell equations. The compression due to electric and magnetic fields are perpendicular to v_d, $P_{E+B} = F_{E+B}/R^2$, the compression pressures. This pressure competes with the escape pressure, P_{es} which equals nkT. The compression due to electric field, $E = k_e N_s q/r'^2$, and the P_E, about $k_e(N_s q)^2/(r'^2 A)$, is the compression pressure of the electric field. The P_B pressure, $N_s q\mathbf{v_d xB}/r^2$, about $\mathbf{JxB}/r^2 = \mu_o/8\pi(I/r)^2$ is the compression pressure of the magnetic field. These two pressures along with surface tension pressure, F_{ST}/m^2, confine the jet plasma contents and overcome the escape pressure, P_{es}. The compression and escape pressures form the conical geometry of the jet plasma in D_2O.

R is the distance, r' or r where the distance r' between the, $^{(+)}$D-O-$D^{(+)}$, hydrogen bonded $D^{(+)}$, a partial charge at the interface of the jet plasma sheath electrons, is used when calculating P_E. The sheath surrounds the jet plasma at the D_2O dielectric surface interface. The average radius of the jet, r, is used when calculating B_E. N_s is the number of electrons in the sheath, n is the density of deuterons (or electrons) in the jet plasma and A is the surface area of the jet. For example, when $N_s = 10^4$ are the number of jet plasma sheath electrons at a density $n = 10^{31}$ the following conditions hold. The jet plasma velocity v_d, $3x10^4$ m/sec; the temperature T, 10_4 ^oK; and the jet plasma geometry (a rod 3 nanometer radius and 90 nanometers in length for simplicity) are all held constant while varying the jet plasma density n.

EM possibility

The motion of the jet plasma in D_2O can be treated as a radiation pressure derived from the cross product of the electric, **E**, and magnetic, **B**, fields not unlike those of electromagnetic waves, EM, except that the fields originate from the motion of electrons in the jet plasma. Along with EM waves and the Poynting vector S, the resulting vector, are in the direction of the jet plasma. Maybe because of the dielectric medium, the force is perpendicular to v_d and some component of the EM waves squeeze the contents of the jet tip to higher densities. The increase may continue until the system becomes degenerate and the jet plasma contents return to D_2O (primary), DOOD, and D_2. It has been noted that densities as high as those of a white dwarf star could be reached.

D_x^+ Cluster; Bosons and Recombination

The jet plasma from the TCB consists of high density deuteron plasma that is further compressed by z-pinch electromagnetic forces. The implantation of deuterons leads to a

situation where deuteron coulombic repulsion would disburse a cluster of thousands of coherent deuterons, D_x^+, before any fusion event could occur.

To counter the apparent short contact time is the following:

The implanted deuterons and electrons in the target lattice need a picosecond of contact time to produce a DD fusion event. To gain this time by extending the time frame of D_x^+, which contains the implanted coherent deuterons, a physical behavior parallel to that of a Cooper electron pair is introduced. The Boson Cooper pair of electrons that exist at low temperatures resists coulomb repulsion forces and is considered as parallel to the possible behavior for deuterons in D_x^+. This environment is at a higher temperature; therefore, the duration of D_x^+ is of a transient nature, perhaps a picosecond, enough contact time to produce a fusion event. This time extension for D^+_x is brought about by the unique system of high density coherent Bosons, BEC, with an overlapping Boson wave function in the D^+_x deuteron cluster.

Another possibility is the parallel to the electron liquid of low temperature and high density origin "Jellium" where the condensed electrons sticky in a Fermi gas surrounded by positive charge do not experience coulomb repulsion. The same condition for deuterons surrounded by electrons in D^+_x will experience reduced coulomb repulsion. These conditions maybe present, but with the high temperature it would transient.

Heat Pulse and Ejecta

The magnitude of the heat pulses are keyed to the sizes of the ejecta that erupt from the cavitation exposed target foil. The sizes of ejecta sites are surveyed via SEM photos of exposed target foils. The jet plasma impact energy of 10^7 particles (deuterons, deuterium atoms, and electrons) into the target foil at $3x10^4$ m/sec is around $4x10^{-8}$ Joules. (and for those that think about micro-meteors, the impact velocity is 30 kilometers per second). There were very few detected ejecta sites or impact sites of this energy size because the implant plasma character leaves little trace of this event. In this regard it is speculated that the highly colored patterns associated with electric fields imposed on target foils are due to their surface plasma implantations. This would be a surface melting process followed by an oxidation via cavitating D_2O. This is similar to a lightning strike on a lattice surface.

Plasma impacts the target, stripping the electrons from the unionized deuterium atoms along with the deuterons, and forms the D_x^+. In the implant process the more mobile electrons penetrate deeper into the lattice than the deuterons, setting up the transient partial charge separation. Electrons, attracted to the exterior deuterons of the D_x^+ from the jet plasma implant, are initially separated from the deuterons. And for a picosecond a recombination process forms deuterium atoms ($D^+ + e^- \rightarrow D$) that squeeze the D_x^+ resisting the coulombic diffusion force and adding their heat of reaction to that locale. There is a long heat pulse that develops from recombination events, perhaps a picosecond in length. One recombination event energy is 10^{-6} that of one fusion event.

A fusion event occurs in the Bosonic cluster of coherent deuterons, D_x^+, creating a spherical heat pulse that, after one nanosecond, erupts from the surface of the target foil with all the fusion products plus the vaporous target foil. These products can be collected and analyzed by MS. The heat pulse for one DD fusion event is 2.6×10^{-11} Joules or 24 Mev per ^{4}He atom, α, produced, and the heat pulse is short, perhaps 10^{-20} seconds or less. The observed SEM ejecta events are about 100 nanometers in diameter for the minimum energy ejecta event and are around 10^{-11} joules or 20 Mev (The ejecta site population maximum in an ejecta event count is done through a SEM photo surface survey). The result of these surveys shows that when comparing the energies of fusion events with recombination events there are million fold differences. The recombination of 1000 deuterons would be 0.0136 Mev and is not significant compared with the 24 Mev of one ^{4}He fusion product let alone a thousand fusion events. The conclusion is that ejecta sites do not have a chemical origin because the recombination heat pulse cannot account for the target foil ejecta sites. Target foil ejecta sites have been found with diameters of 1600 nanometers and are equivalent to as many as 10^4 fusion events or 10^{10} recombinations and this not possible. The target foils go through billions of heating and cooling cycles destroying earlier local melted sites with newly formed sites while the target foil is slowly being degraded.